Calhoun
Institutional Archive of the Naval Postgraduate School

Calhoun: The NPS Institutional Archive

DSpace Repository

Theses and Dissertations 1. Thesis and Dissertation Collection, all items

1990-06

Analysis of radio frequency radiation from a propagating electron beam

Lally, Richard W.

Monterey, California. Naval Postgraduate School

http://hdl.handle.net/10945/37527

This publication is a work of the U.S. Government as defined in Title 17, United States Code, Section 101. Copyright protection is not available for this work in the United States.

Downloaded from NPS Archive: Calhoun

DUDLEY
KNOX
LIBRARY

http://www.nps.edu/library

Calhoun is the Naval Postgraduate School's public access digital repository for research materials and institutional publications created by the NPS community. Calhoun is named for Professor of Mathematics Guy K. Calhoun, NPS's first appointed -- and published -- scholarly author.

Dudley Knox Library / Naval Postgraduate School
411 Dyer Road / 1 University Circle
Monterey, California USA 93943

AD-A237 941

NAVAL POSTGRADUATE SCHOOL
Monterey, California

DTIC
ELECTE
JUL 11 1991
S C D

THESIS

ANALYSIS OF RADIO FREQUENCY RADIATION FROM A PROPAGATING ELECTRON BEAM

by

Richard W. Lally

June 1990

Thesis Advisor: John R. Neighbours

Approved for public release; distribution is unlimited.

91-04494

91 7 09 068

Unclassified
SECURITY CLASSIFICATION OF THIS PAGE

REPORT DOCUMENTATION PAGE

Form Approved OMB No. 0704-0188

1. REPORT SECURITY CLASSIFICATION: Unclassified

1b. RESTRICTIVE MARKINGS

2a. SECURITY CLASSIFICATION AUTHORITY

2b. DECLASSIFICATION/DOWNGRADING SCHEDULE

3. DISTRIBUTION/AVAILABILITY OF REPORT: Approved for public release; distribution is unlimited

4. PERFORMING ORGANIZATION REPORT NUMBER(S)

5. MONITORING ORGANIZATION REPORT NUMBER(S)

6a. NAME OF PERFORMING ORGANIZATION: Naval Postgraduate School

6b. OFFICE SYMBOL *(If applicable)*: 33

7a. NAME OF MONITORING ORGANIZATION: Naval Postgraduate School

6c. ADDRESS *(City, State, and ZIP Code)*: Monterey, CA 93943-5000

7b. ADDRESS *(City, State, and ZIP Code)*: Monterey, CA 93943-5000

8a. NAME OF FUNDING/SPONSORING ORGANIZATION

8b. OFFICE SYMBOL *(If applicable)*

9. PROCUREMENT INSTRUMENT IDENTIFICATION NUMBER

8c. ADDRESS *(City, State, and ZIP Code)*

10. SOURCE OF FUNDING NUMBERS

PROGRAM ELEMENT NO.	PROJECT NO.	TASK NO.	WORK UNIT ACCESSION NO.

11. TITLE *(Include Security Classification)*: Analysis of Radio Frequency Radiation from a Propagating Electron Beam

12. PERSONAL AUTHOR(S): Richard W. Lally

13a. TYPE OF REPORT: Master's Thesis

13b. TIME COVERED: FROM ________ TO ________

14. DATE OF REPORT *(Year, Month, Day)*: June 1990

15. PAGE COUNT: 94

16. SUPPLEMENTARY NOTATION: The views expressed in this thesis are those of the author and do not reflect the official policy or position of the Department of Defense or the U.S. Government.

17. COSATI CODES

FIELD	GROUP	SUB-GROUP

18. SUBJECT TERMS *(Continue on reverse if necessary and identify by block number)*: Cherenkov Radiation, Transition Radiation, EMP, Radio Frequency Radiation, Electron Beam

19. ABSTRACT *(Continue on reverse if necessary and identify by block number)*

An experiment was conducted which measured the Radio Frequency (RF) radiation from the PHERMEX accelerator, capable of 30 MeV and 600 A. This was accomplished by placing TEM horn antennae at varying angles from the path of the electron beam. The signals received by the antennae were then recorded by using a Digitizing Camera System (DCS). Measurements were taken of the radiation from propagating and non-propagating beams, beams with energy above and below Cherenkov threshold, and beams with varied currents. The captured RF signals and their corresponding frequency spectra were then analyzed. This analysis showed that the radio frequency radiation from the beams below the Cherenkov threshold contained primarily transition radiation; when above, diffracted Cherenkov radiation was observed. Non-propagating beams produced larger-angle radiation and had less definition in their spectrum. All electric fields measured were proportional to the beam current. Lastly, the electron beam pulse width and separation were determined by both the received signals and their spectrum.

20. DISTRIBUTION/AVAILABILITY OF ABSTRACT: ☒ UNCLASSIFIED/UNLIMITED ☐ SAME AS RPT. ☐ DTIC USERS

21. ABSTRACT SECURITY CLASSIFICATION: Unclassified

22a. NAME OF RESPONSIBLE INDIVIDUAL: John R. Neighbours

22b. TELEPHONE *(Include Area Code)*: (408) 646-2922

22c. OFFICE SYMBOL: 61 Nb

DD Form 1473, JUN 86 *Previous editions are obsolete*

SECURITY CLASSIFICATION OF THIS PAGE
Unclassified

Approved for public release; distribution is unlimited.

Analysis of Radio Frequency Radiation from a Propagating Electron Beam

by

Richard W. Lally
Captain, United States Army
B.S., Stonehill College, 1979

Submitted in partial fulfillment of the
requirements for the degree of

MASTER OF SCIENCE IN PHYSICS

from the

NAVAL POSTGRADUATE SCHOOL
June 1990

Author: [redacted]
Richard W. Lally

Approved by: [redacted]
John R. Neighbours, Thesis Advisor

[redacted]
Fred R .Buskirk, Second Reader

[redacted]
Karlheinz E. Woehler, Chairman,
Department of Physics

ABSTRACT

An experiment was conducted which measured the Radio Frequency (RF) radiation from the PHERMEX accelerator, capable of 30 MeV and 600 A. This was accomplished by placing TEM horn antennae at varying angles from the path of the electron beam. The signals received by the antennae were then recorded by using a Digitizing Camera System (DCS). Measurements were taken of the radiation from propagating and non-propagating beams, beams with energy above and below Cherenkov threshold, and beams with varied currents. The captured RF signals and their corresponding frequency spectra were then analyzed. This analysis showed that the radio frequency radiation from the beams below the Cherenkov threshold contained primarily transition radiation; when above, diffracted Cherenkov radiation was observed. Non-propagating beams produced larger-angle radiation and had less definition in their spectrum. All electric fields measured were proportional to the beam current. Lastly, the electron beam pulse width and separation were determined by both the received signals and their spectrum.

Accession For
NTIS GRA&I ☑
DTIC TAB ☐
Unannounced ☐
Justification
By
Distribution/
Availability Codes

Dist	Avail and/or Special
A-1	

TABLE OF CONTENTS

I. **INTRODUCTION** 1

A. BACKGROUND 1

1. Historical Look at Cherenkov Radiation 1
2. Cherenkov and Diffracted Cherenkov Radiation Theory .. 3
3. Transition Radiation Theory 6
4. Comparison of Diffracted Cherenkov and Transition Radiation 8

B. PREVIOUS EXPERIMENTS 9

C. PURPOSE 10

II. **EXPERIMENTAL APPROACH** 11

A. EQUIPMENT ARRANGEMENT 11

B. ACCELERATOR AND BEAM CHARACTERISTICS 11

C. ANTENNA CHARACTERISTICS 14

D. DESCRIPTION OF DIGITIZING CAMERA SYSTEM (DCS) 15

E. ANTENNA PLACEMENT 16

F. DATA ACQUISITION 16

1. Beam Adjustment 16
2. Waveform Capture by DCS 20

III. DATA REDUCTION 21
- A. DATA FILE CONVERSION AND TRANSFER 21
- B. INTERACTIVE DATA LANGUAGE (IDL) PROGRAM APPLICATION 21
- C. ANTENNA RESPONSE 22
- D. SIGNAL REPRODUCIBILITY 28
- E. ANTENNA-TO-ANTENNA COMPARISON 28

IV. RESULTS AND DISCUSSION 32
- A. RESULTS 32
  - 1. Signals and Related Spectrum 32
  - 2. Signal Strength as a Function of Angle 32
  - 3. Relative Intensity of Spectrum Harmonics 45
  - 4. Harmonic Frequency Shift 46
  - 5. Modulation of Spectrum 57
- B. DISCUSSION 62
  - 1. Signals and Related Spectrum 62
  - 2. Signal Strength as a Function of Angle 63
  - 3. Relative Intensity of Spectrum Harmonics 64
  - 4. Harmonic Frequency Shift 65
  - 5. Modulation of Spectrum 65

V. CONCLUSIONS 67

APPENDIX A EQUIPMENT LIST 69

APPENDIX B IDL ANALYSIS PROGRAM 70

LIST OF REFERENCES 77

INITIAL DISTRIBUTION LIST 79

LIST OF TABLES

1 Data Collection Summary 18

2 Antenna Conversion 30

3 Actual Beam Currents (in amps) 45

4 Comparison of Actual to Expected Electric Field 46

5 Modulation Minima 62

LIST OF FIGURES

1. Envelope Function for Beam Parameters 5
2. Frequency Shifting with Angle 6
3. Transition Energy Emitted per Unit Angle 8
4. Radiation Areas with a Finite Beam 10
5. Equipment Arrangement 12
6. Collection System 13
7. Schematic of Phermex Accelerator 14
8. Schematic of TEM Horn Antenna 15
9. Antenna Placement 17
10. Antenna Placement 18
11. Typical B Dot Signal 19
12. Example of Program Output 23
13. Antenna Response 24
14. Antenna Response 24
15. Comparison of Correction Values 26
16. Antenna A & B1 Transfer Functions 27
17. Reproducible Signals from Antenna A 29
18. Reproducible Signals from Antenna B1 29
19. Comparison of Antenna A and B1 Signals 30
20. Signal and Spectrum for Full Current, Angles of 5 and 10 Degrees 33
21. Signal and Spectrum for Full Current, Angles of 15 and 30 Degrees 34

22. Signal and Spectrum for Full Current, Angles of 45 and 60 Degrees 35
23. Signal and Spectrum for Half Current, Angles of 5 and 10 Degrees 36
24. Signal and Spectrum for Half Current, Angles of 15 and 30 Degrees 37
25. Signal and Spectrum for Half Current, Angles of 45 and 60 Degrees 38
26. Signal and Spectrum for Diffuse Beam, Angles of 5 and 10 Degrees 39
27. Signal and Spectrum for Diffuse Beam, Angles of 15 and 30 Degrees 40
28. Signal and Spectrum for Diffuse Beam, Angles of 45 and 60 Degrees 41
29. Signal and Spectrum for Half Energy Beam, Angles of 5 and 10 Degrees 42
30. Signal and Spectrum for Half Energy Beam, Angles of 15 and 30 Degrees 43
31. Signal and Spectrum for Half Energy Beam, Angles of 45 and 60 Degrees 44
32. Signal Strength of Full Versus Half Current 47
33. Signal Strength of Tight Versus Diffuse Beam 48
34. Signal Strength of Full Versus Half Energy 49
35. Ratio of Full to Half Current Signals 50
36. Ratio of Tight to Diffuse Beam Signals 50
37. Ratio of Full to Half Energy Beam Signals 51
38. First Four Harmonics of Half Current Spectrum 52
39. First Four Harmonics of Diffuse Beam Spectrum 53

40. First Four Harmonics of Half Energy Spectrum 54
41. First Four Harmonics of Full Current Spectrum 55
42. 5-9 Harmonics of Full Current Spectrum 56
43. Average Frequency of Spectrum for Full Current 57
44. Average Frequency of Spectrum for Half Current 58
45. Average Frequency of Spectrum for Full Current B Dot 58
46. Average Frequency of Spectrum for Half Current B Dot 59
47. Signal and B Dot Difference for Full Current 59
48. Signal and B Dot Difference for Half Current 60
49. Modulation Example from a Perfectly Pulsing Accelerator 61

ACKNOWLEDGMENTS

I wish to express my gratitude and appreciation to Professor John R. Neighbours and Professor Fred R. Buskirk for the opportunity to explore this topic. Their advice and guidance have made this an interesting as well as enjoyable experience.

Also, a special thanks to Dr. David Moir of Los Alamos National Laboratory for his assistance and advice on PHERMEX, both during and after the experiment.

In addition, the technical assistance provided by Mr. Donald Snyder on the operation and the set-up of the equipment was greatly appreciated.

Finally, but foremost, I wish to thank my wife, Gina, for her endless patience, care, and support for me and our three wonderful daughters, Kacie, Kristen, and Erin.

I. INTRODUCTION

A. BACKGROUND

1. Historical Look at Cherenkov Radiation

The following history of Cherenkov radiation discovery and development is based on Jelley's introduction [Ref. 1] and follows the summary by O'Grady [Ref. 2].

As early as 1910, the effects of Cherenkov radiation were observed by Mme. Curie. Her bottles of concentrated radium solution emitted a pale blue light. This phenomenon was subsequently partially investigated by Mallet during the years between 1926 and 1929. However, it was not until 1938 that Cherenkov commenced an exhaustive series of experiments to fully understand this phenomenon. During this time, a theory was proposed by Frank and Tamm which had excellent agreement with Cherenkov's experimental results. Since their work, there have been numerous theories and experiments concerning Cherenkov radiation detection and Cherenkov radiation applications.

By Frank and Tamm's definition [Ref. 3], Cherenkov radiation takes place when a charged particle moves at a constant velocity which is larger than the phase velocity of light in a transparent medium. Electrons can be accelerated to speeds greater than the velocity of light in air and thus produce Cherenkov radiation. Frank and Tamm's theory, however, contains a number of simplifying assumptions. Two of the more important assumptions are that the medium is an unbounded continuum and the track length is infinite [Ref. 1]. Applying these assumptions to most accelerator applications is unrealistic. When an electron bunch leaves the vacuum of an accelerator, another medium (such as air) is encountered. The electron beam steadily loses energy due to ionization of air molecules. Therefore, the beam has a finite length and propagates in a bounded medium.

When the two previously made assumptions are violated, two similar types of radiation occur—diffracted Cherenkov radiation and transition radiation [Ref. 4]. Diffracted Cherenkov radiation is caused by the finite beam interaction length and transition radiation is caused by a boundary where the index of refraction of the medium changes. Another type of radiation closely related to transition radiation is diffracted transition radiation [Ref. 5]. In this case, radiation is produced when a charged particle passes through an aperture or travels near any interface between differing media. The circular beam port of an accelerator is an obvious source of diffracted transition radiation. However, since the circular beam port dimensions are constant, the resulting radiation will merely be added to the transition radiation and considered the electromagnetic pulse (EMP).

Since the major effects of this experiment concern both EMP and diffracted Cherenkov, a more-detailed summary for each is contained in the following two sections. The last section in this chapter addresses the similarities and differences of both.

2. Cherenkov and Diffracted Cherenkov Radiation Theory

As previously stated, Cherenkov radiation is produced whenever a charged particle travels through a dielectric medium faster than the phase velocity of light in the same medium. The underlying reason radiation forms is that the charged particle temporarily excites the medium. The ionized molecules briefly radiate as a dipole. Of particular interest is the Cherenkov angle θ_C. When the interaction length is infinite, the radiation propagates only at this angle. The Cherenkov angle can be calculated using

$$\cos \theta_C = \frac{c}{nv} \tag{1}$$

where c is the speed of light in a vacuum, n is the refractive index of the medium, and v is the speed of the particle. A more-detailed description of Cherenkov radiation and a thorough derivative of the fundamental equation for output of radiation is given by Jelley [Ref. 1]. However, since θ_C occurs at approximately one degree, the diffracted Cherenkov radiation will be more applicable to this experiment.

Measurements by Neighbours, Buskirk, and Saglam [Ref. 6] in 1983 showed that the Cherenkov cone angle is broader as the interaction length is decreased from infinity. This, of course, is diffracted Cherenkov radiation. Neighbours, Buskirk, and Saglam [Ref. 7] derive an equation for the total coherent power per unit solid angle, radiated at the frequency ν by a periodic charged particle beam traveling a finite distance L at constant velocity. This equation is

$$w(\nu,k) = \nu_o^2 Q R^2 \quad (2)$$

where ν_0 is the fundamental frequency of the beam generator and where the constant Q is

$$Q = \frac{\mu c q^2}{8\pi^2}$$

where μ is the permeability of the medium and q is the change in the electron bunch. The radiation function R is given by:

$$R = w\pi\eta \sin\theta \, I(u) F(k) \quad (3)$$

where:

θ = angle between emitted radiation and beam path
η = L/λ
L = beam interaction length
λ = radiation wavelength
$F(k)$ = dimensionless form factor
$I(u)$ = $\sin u/u$ = diffraction function

where u is:

$$u = \pi\eta[\cos\theta_c - \cos\theta] \quad (4)$$

A graph of equation 3 with the appropriate constants for this experiment yields Figure 1. This envelope function determines the relative output power for a given angle from the beam path.

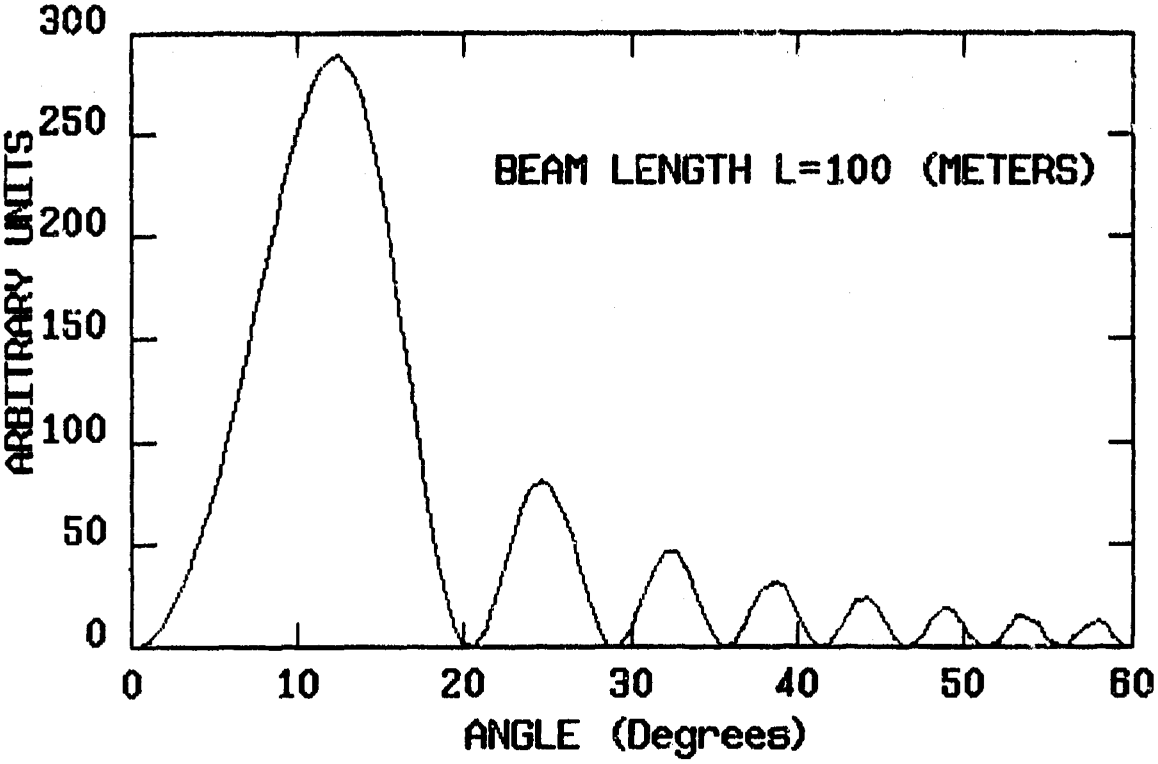

Figure 1. **Envelope Function for Beam Parameters**

Two additional comments concerning diffracted Cherenkov radiation are: (1) "the power emitted for coherent radiation is proportional to the source of the beam current" [Ref. 8]. (2) Neighbours, Buskirk, and Maruyama [Ref. 9] also predict that "the oscillations of the frequency distribution of the radiation are of increasing "frequency" as the angle of propagation moves toward the back direction." To better understand this statement, one should view Figure 2 (obtained from Reference 9). From Figure 2, the predicted pattern is clear.

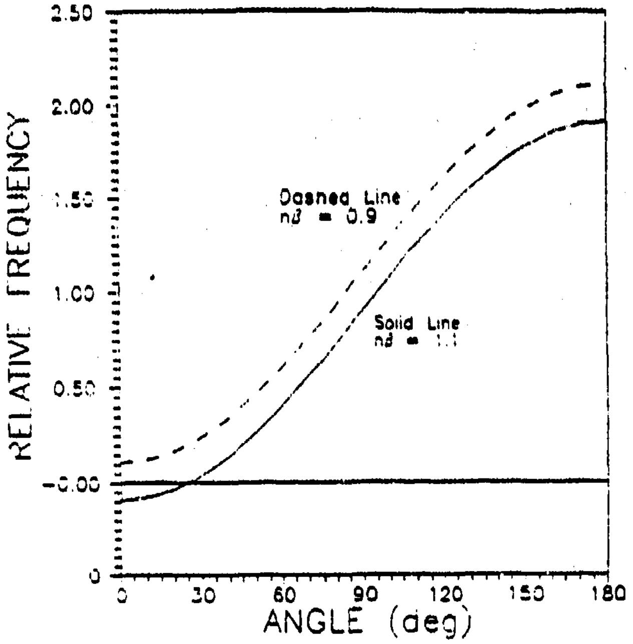

Figure 2. **Frequency Shifting with Angle**

3. Transition Radiation Theory

While Cherenkov radiation occurs when the velocity of the particle is greater than the speed of light in that medium, transition radiation can occur whether the beam energy is above or below the Cherenkov threshold energy. When the electron passes through a boundary between two different media transition radiation is produced. Frank and Ginsburg [Ref. 10] explain the nature of this phenomenon by considering the transition of an electron from a vacuum into a perfect conductor. While the electron moves in the vacuum, there is no radiation. However, the field in the vacuum is equal to the field of the electron and its image moving toward it. Once the electron exits the vacuum, both the electron and its image cease to exist from the vacuum field perspective. Therefore, radiation must be given off in much the same way as it is emitted when an electron suddenly stops.

Work done by Buskirk and Neighbours [Ref. 4] develops a useful equation by which the electric and magnetic field strengths can be evaluated. The maximum magnetic field is given by

$$B = \beta \frac{\sin\theta}{R} I_o \frac{1}{1-\beta\cos\theta}$$

where θ is the angle between the beam path and detection point, R is the distance between the field point and the beam port, and I_0 is the current of the accelerator. The constant β is defined to be

$$\beta = \frac{v}{c} = \frac{v}{c_o} \cdot n,$$

where c is the velocity of radiation in the median, c_0 is the velocity of light in free space, and n is the index of refraction of the medium. For this experiment, the transition will be from vacuum to air as the electron bunch leaves the accelerator. The electric field can therefore be written as [Ref. 11]

$$E = \frac{c\omega_o}{4\pi} \frac{\sin\theta}{R} I_o \frac{1}{1-\beta\cos\theta} \tag{6}$$

where ω_0 is the permeability of free space. Figure 3 [Ref. 11] shows the relation between transition energy emitted per angle as a function of beam energy.

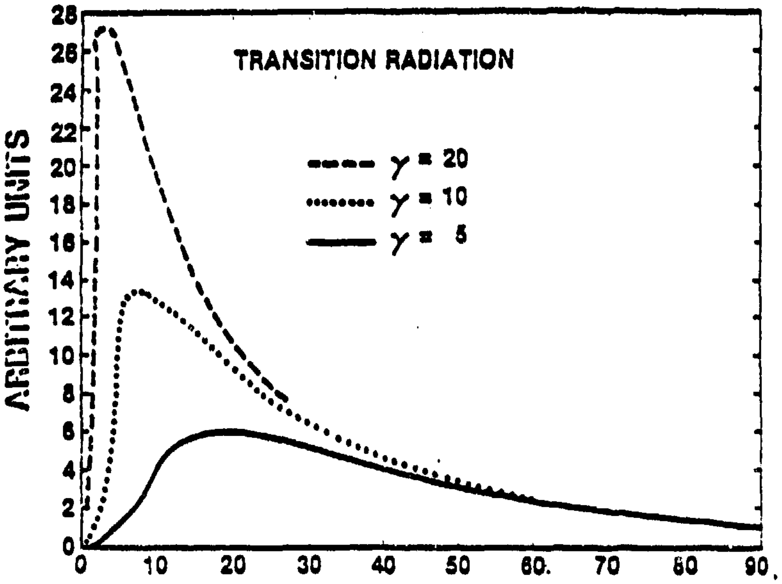

Figure 3. **Transition Energy Emitted per Unit Angle**

Diffraction radiation during this experiment will be measured and treated as additional transition radiation.

4. Comparison of Diffracted Cherenkov and Transition Radiation

The similarities between Cherenkov and transition radiation were summarized by Buskirk, Mack, and Neighbours [Ref. 12]. First, both radiation fields are polarized, with the electric field in the plane of the observer and the beam path, and the magnetic field perpendicular to that plane. Also, the electric field pulse qualitatively follows the current pulse. Last, the field from either diffracted Cherenkov or transition is proportional to the beam current. Therefore, the radiated power is proportional to the current squared.

There are, however, some important differences between Cherenkov and transition radiation. Transition radiation is concerned with transiting boundaries. Boundaries associated with electron accelerators are the beam port and beam stops. Although data was taken with beam stops in position, they will be analyzed in a follow-on experiment. The next difference is that Cherenkov radiation occurs in air when the beam energy is above the Cherenkov threshold. Also, the Cherenkov power radiated (without diffraction) is proportional to the path length. Figure 4 [Ref. 4] shows two regions: A and B. Cherenkov radiation (without diffraction) is concentrated at one angle (region B). With diffraction, radiation spreads out about the Cherenkov angle θ_c, whereas transition radiation occurs at all angles (regions A and B) with increased intensity in the forward direction.

B. PREVIOUS EXPERIMENTS

There have been a number of experiments conducted which measure optical, x-ray, or microwave radiation from electron beams. However, relatively few experiments have measured radio frequency radiation from propagating electron beams. Buskirk and Neighbours have previously performed a number of such experiments [Ref. 13] dealing with radio frequency radiation. The present experiment differs from their earlier efforts in the following ways: (1) the number of angles at which data were sampled was increased, (2) many measurements were recorded with varied beam parameters, and (3) most importantly, a digitizing camera was incorporated into the collection system. This provided a quicker and

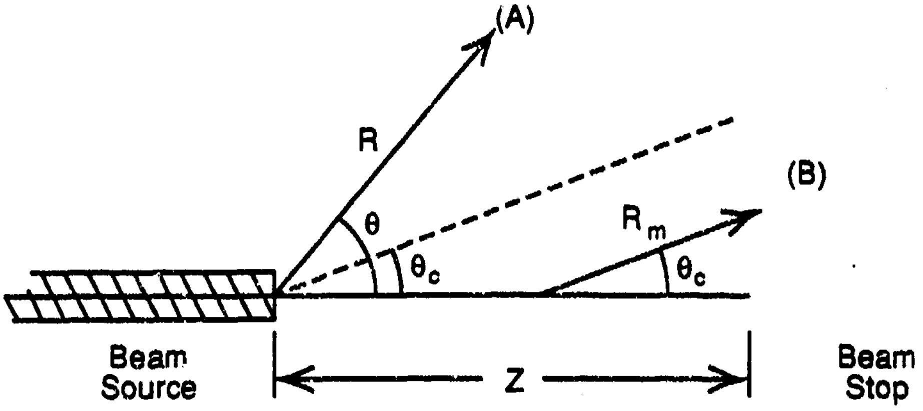

Figure 4. **Radiation Areas with a Finite Beam**

easier method for data collection and storage. This digitizing camera also has another important advantage over the previous analog system. The resulting data files can be analyzed by computer programs and software without painful conversions.

C. PURPOSE

The general overall objective is similar to that of earlier experiments: to understand the radio frequency radiation produced by an intense electron beam. More specifically, the purpose of this experiment can be defined in the following statements:

1. Observe differences in propagating to non-propagating beams by varying the beam focus.
2. Attempt to isolate diffracted Cherenkov radiation effect from electromagnetic pulse (EMP) by varying the beam energy above and below the Cherenkov threshold (about 20 MeV).
3. Observe possible instabilities in beam propagation due to high currents. Conversely, investigate the effect low current has on pinching the beam.
4. Analyze the radiation signal and frequency spectrum for empirical observations.

II. EXPERIMENTAL APPROACH

A. EQUIPMENT ARRANGEMENT

The specific equipment used in this experiment is listed in Appendix A. In order to collect data simultaneously from two antennae and also obtain the original source signal, three independent collection systems were required. The equipment arrangement for one of the antennae collection systems can be seen in Figure 5. The collection system for the source signal is essentially the same, except that one of the accelerator's B dot loops at the beam port replaces the antenna. Actual pictures of the collection systems (minus the antennae) are seen in Figure 6. In this setup, the radiation from the electron beam is received by the TEM horn antenna and transmitted to the oscilloscope by means of the double-shielded transmission cable. The signal on the oscilloscope is digitized by a Digitizing Camera System (DCS) and stored on a computer. The B dot loop signal was recorded in a similar fashion and was also used to trigger the other two oscilloscopes.

B. ACCELERATOR AND BEAM CHARACTERISTICS

The accelerator used to produce the electron beam was PHERMEX, located at Los Alamos National Laboratory (LANL), New Mexico. A schematic of PHERMEX (Figure 7) shows the three cavities which are excited by means of radio frequency amplifiers operating at 50 MHz. PHERMEX can produce a 30 MeV, 900 A beam focused to a 6 mm

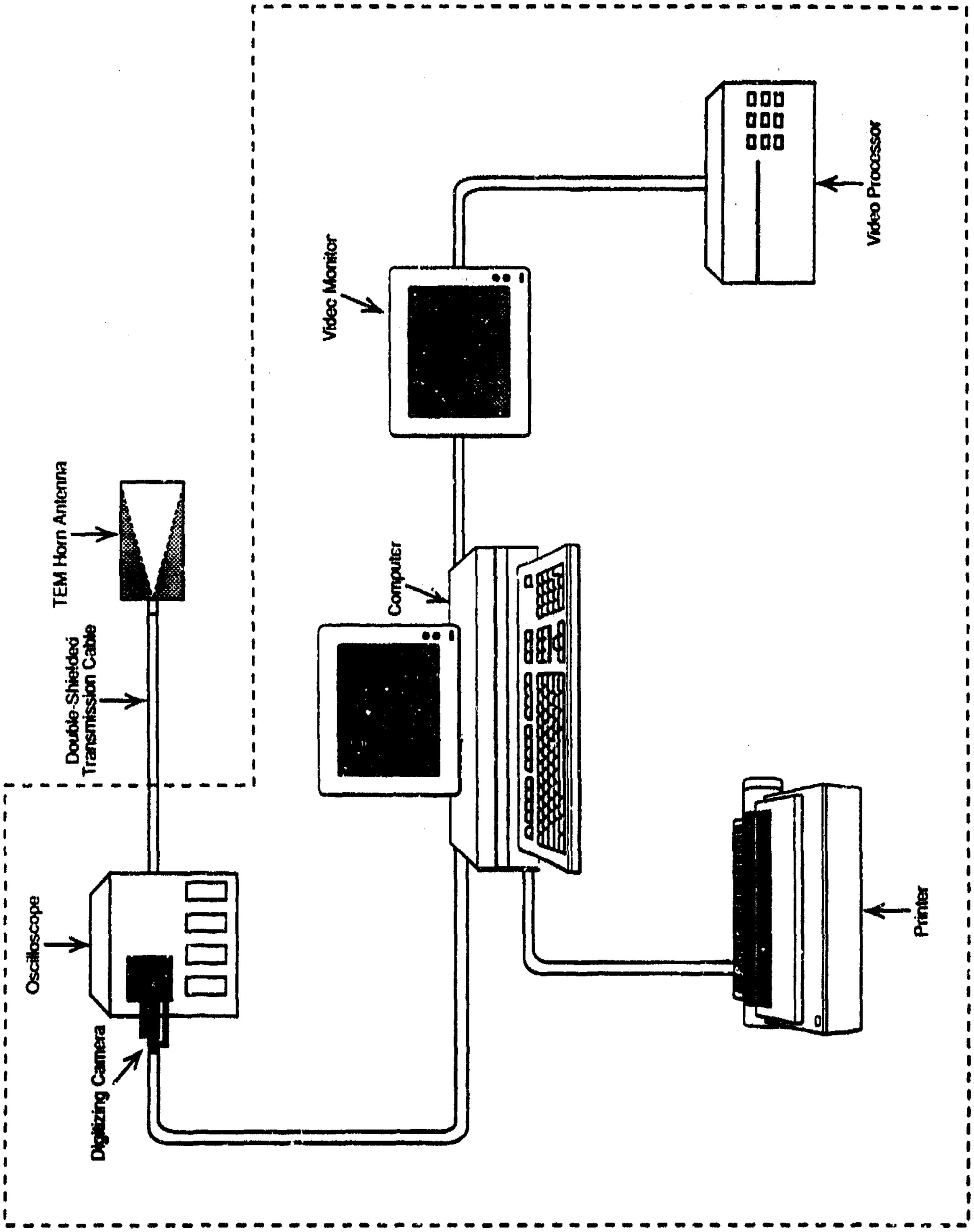

Figure 5. **Equipment Arrangement**

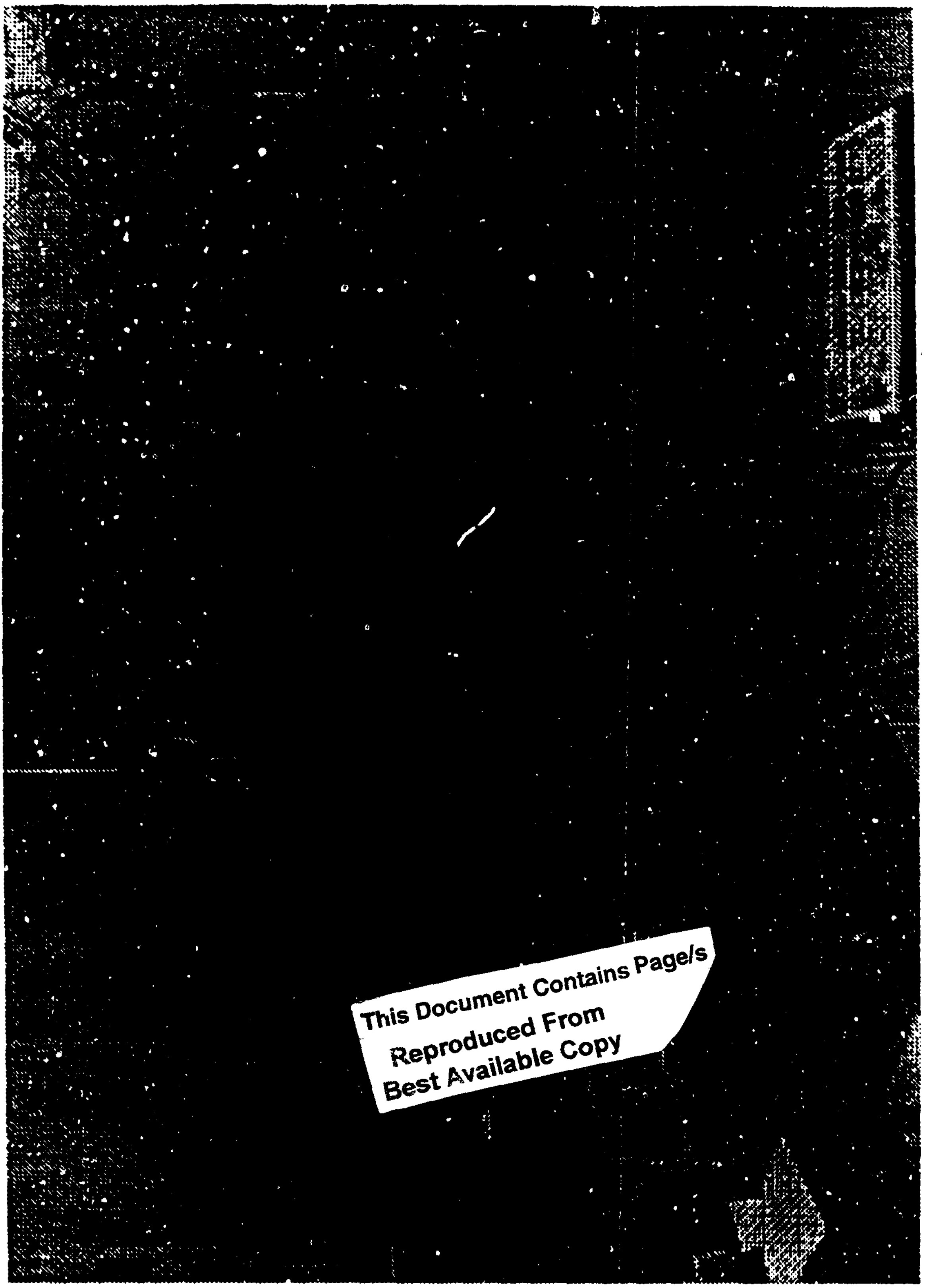

This Document Contains Page/s Reproduced From Best Available Copy

Figure 6. **Collection System**

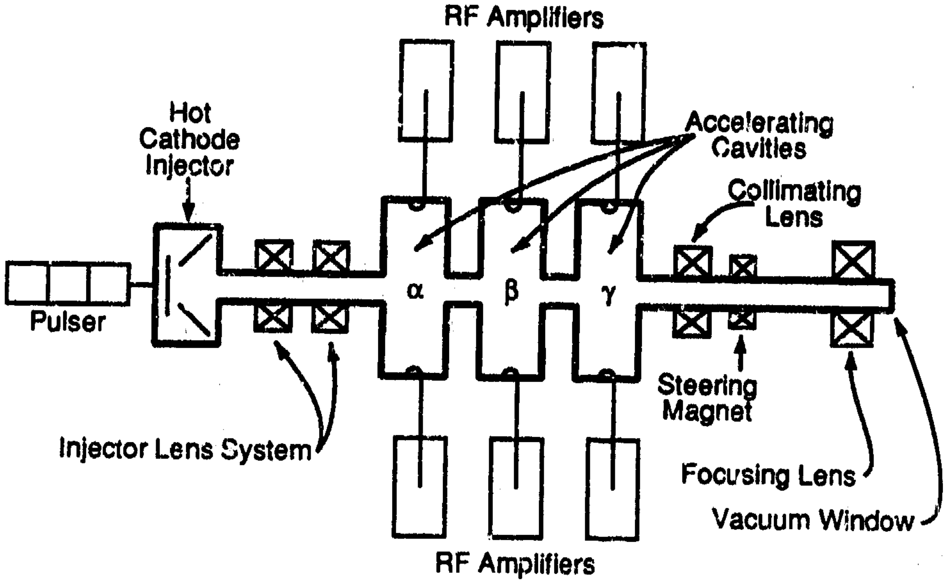

Figure 7. **Schematic of Phermex Accelerator**

diameter. The energy, current, and diameter can be varied as required (see Beam Adjustment section). The pulse train created by PHERMEX is a maximum of 10 pulses, two to three nanoseconds (ns) long, and separated by 20 ns. Pulse trains can be formed up to one per minute [Ref. 14].

C. ANTENNA CHARACTERISTICS

The transverse electromagnetic (TEM) horn antenna was developed at the National Bureau of Standards[Ref. 15]. The horn is configured as a two-conductor, end-fire, traveling-wave structure. Continuously tapered resistive loading of the two conductive elements provides a relatively short, broadband, nondispersive antenna which has high directivity. Sections of polystyrene foam support the horn's resistively tapered conductors. The antenna is enclosed in a bakelite box which measures about 30 cm wide by 15 cm high by 51 cm long. A schematic of the antenna is shown in Figure 8. The antenna can measure electric fields between 1 and 1,600 $\frac{V}{M}$ from 1 MHz to 15 GHz, with a flatness of ±2 dB [Ref. 16].

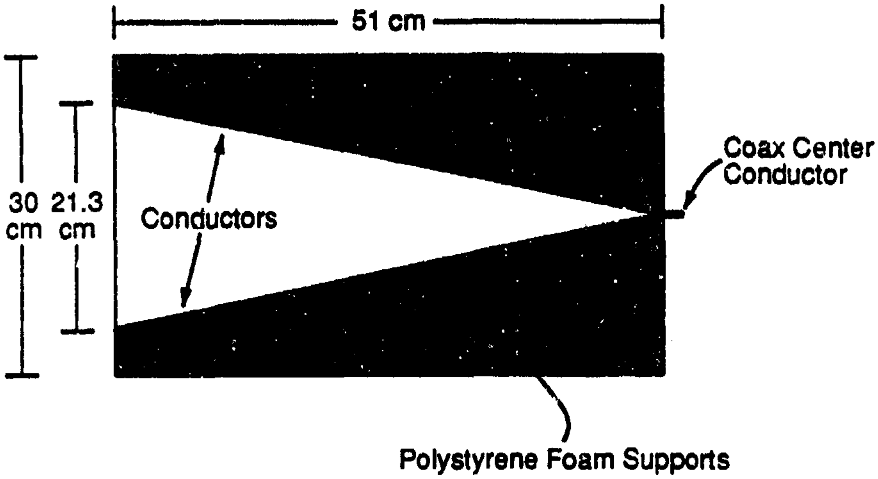

Figure 8. **Schematic of TEM Horn Antenna**

D. DESCRIPTION OF DIGITIZING CAMERA SYSTEM (DCS)

The Tektronix DCS [Ref. 17] is a charge-coupled device (CCD) camera which connects directly to the face of the oscilloscope. 490 vertical by 384 horizontal picture elements are used to form an image of the trace on the oscilloscope. Then the camera transfers the analog video signal to the frame store board. The frame store board is a General Purpose Information Bus (GPIB) located in an IBM-compatible computer. The conversion from analog video signal to digital format is performed by the frame storage board. Here, the digitized raw image which is held in the computer's temporary memory can then be stored on diskettes or a hard disk. The

DCS software, along with the frame store board, allows for format conversion, wave form manipulation, and file transfer. Williams provides a more-detailed summary of the DCS system and software [Ref. 18].

E. ANTENNA PLACEMENT

The two antennae were each mounted on top of eight-foot ladders. At this height, the antennae were approximately two and a half feet higher than the beam port. Figure 9 shows one of the actual antenna placements. However, in this picture, both antennae are mounted on the same ladder. The positioning of each antenna was relative to the beam path from the beam port. At a constant radius of 90 feet, six positions (5-, 10-, 15-, 30-, 45-, and 60-degree angles) relative to the beam path were measured and marked. A schematic of the antenna placements is seen in Figure 10. Permanent structures on one side of the beam path prevented measurements in that direction.

F. DATA ACQUISITION

1. Beam Adjustment

Radiation from the electron beam was recorded in sets of three to five signals per antenna angular position. This procedure was carried out to form specific groups comprised of four variations of the electron beam (see Table 1). The first group of data sets was taken at full current (510 A) and full energy (29.5 MeV). The beam was focused to 6 mm for all shots in this group. The second group consisted of data sets received

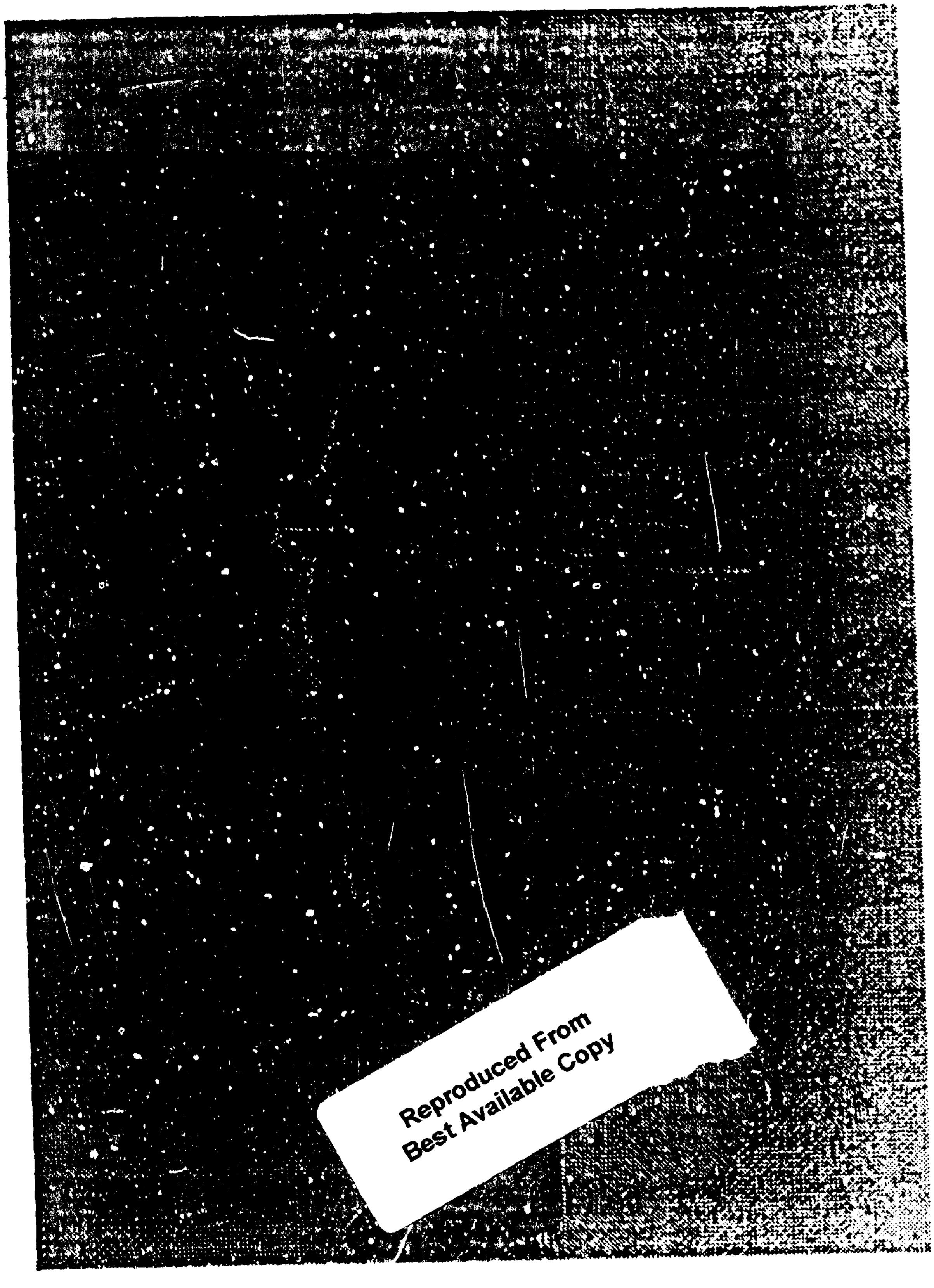

Figure 9. **Antenna Placement**

Reproduced From
Best Available Copy

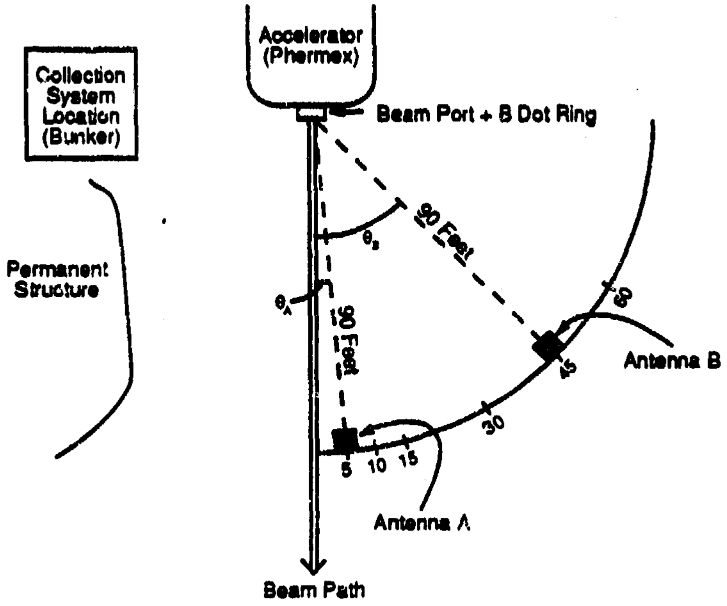

Figure 10. **Antenna Placement**

TABLE 1

DATA COLLECTION SUMMARY

			Angles (Degrees)					
Group	**Beam Parameters**	**Antenna**	**5**	**10**	**15**	**30**	**45**	**60**
1	Full Current & Full Energy & Tight	A	X	X	X	X		
		B1		X		X	X	X
2	Half Current & Full Energy & Tight	A	X	X	X			
		B1				X	X	X
3	Full Current & Full Energy & Diffuse	A	X	X	X			
		B2				X	X	X
4	Half Current & Half Energy & Tight	A	X		X	X	X	X
		B2	X	X	X	X	X	X

with the beam at half current (300 A). All other parameters of the beam remained fixed. The third group of data sets was altered only by the diameter of the beam. The accelerator's focusing magnet was adjusted to deliver a diffused or under-focused beam. In the last group, a half-energy (15 MeV), half-current, focused beam produced the signals.

Throughout all of the shots in this experiment, the pulse train remained at either six or seven pulses with a pulse width of 3.5 ns and a pulse separation of 20 ns (see Figure 11). Therefore, the pulse trains varied from 121 to 145 ns.

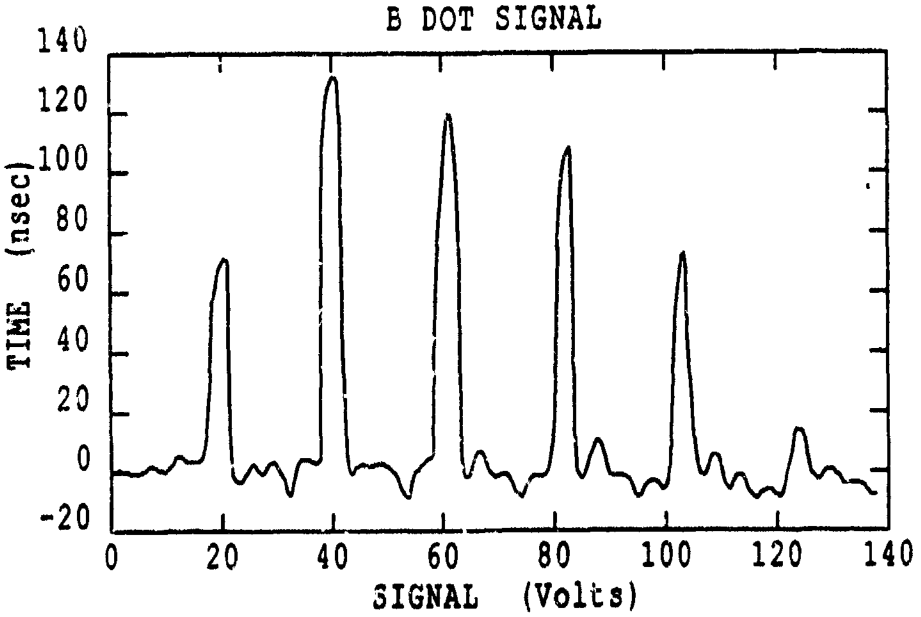

Figure 11. **Typical B Dot Signal**

The current of the beam can be determined from the maximum peak value. The beam current I is related to the peak voltage V, by

$$I = C_I V \tag{7}$$

where $C_I = 129$ A/V, V is in volts, and I is in amps [Ref. 14].

Current, pulse shape, and number of pulses varied from day to day, but consecutive shots were fairly reproducible.

2. Waveform Capture by DCS

The radiation signal received by the antenna was transmitted to the oscilloscope by means of the shielded coaxial cable. The image displayed on the oscilloscope was automatically captured by the DCS. The signal captured by the camera was immediately digitized by the frame store board. The original analog signal was displayed on a TV monitor while the digitized signal was graphed on the computer monitor. Prior to each Phermex shot, the current oscilloscope settings and intended waveform/file name for each waveform were input into the Compaq computer by use of the DCS software. Each waveform was saved on the hard disk of the respective computer and a second copy of each file was preserved on diskette.

III. DATA REDUCTION

A. DATA FILE CONVERSION AND TRANSFER

The waveforms were recorded and saved in a binary format. Since binary is the normal format when viewing the computer display and binary requires less disk storage, this was the preferred format. As previously mentioned, various waveform manipulations can be accomplished using the DCS software in the binary format. However, some waveform manipulations such as the Fast Fourier Transform (FFT) cannot be performed with the DCS software. A VAX system was selected to handle the additional waveform manipulations. Therefore, an ASCII file format was desirable. Nine hundred and seventy-five (975) binary-formatted files were individually converted to an ASCII format using the DCS software's built-in feature. During this process, each file was coded with an eight-digit file name to provide the maximum information pertaining to the signal's capture parameters.

Once reformatted and coded, all files were transferred from the IBM-compatible computer to the VAX system. A KERMIT software program provided the means for transferring the files. The VAX system used was a Digital Microvax computer

B. INTERACTIVE DATA LANGUAGE (IDL) PROGRAM APPLICATION

A program, written with Interactive Data Language (IDL) [Ref. 19] on the VAX system, was developed to analyze the collected waveforms. Appendix B contains a copy of the main (modified) analysis program.

This program corrects for the required in-line attenuation, the antenna response function, and the DC offset. Once the corrections are made, the radiation signal and the FFT of the signal are plotted. Directly to the right of these plots, the corresponding B dot signal and its FFT are depicted. Figure 12 is an example of the program's output. This program was run in a batch mode to produce graphs for all the radiation signals. To obtain additional information, the program was modified to be user-interactive. This interactive program allows the user to truncate the radiation or B dot signal to the exact start and finish of the signal. In addition, the program will compile the peak frequencies of the FFT and their corresponding relative intensities.

C. ANTENNA RESPONSE

Two of the three TEM horns, A and B1, were calibrated by the National Bureau of Standards (NBS). Two sets of responses for each TEM horn were tabulated. Each print-out of the data set consisted of 101 points. The first set contained responses from 50 MHz to 5 GHz at 50 MHz intervals and a graph of the data (Figure 13). The second set consisted of responses from 1 MHz to 101 MHz at 1 MHz intervals and a graph of the responses from 1 MHz to 512 MHz (Figure 14). The overall uncertainty of the calibration is ±1.0 dB.

A print-out with the response for every MHz from 1 MHz to 600 MHz would have been ideal. However, an attempt was made using the second set's graph (Figure 14) to extract the response from 5 MHz to 512 MHz at

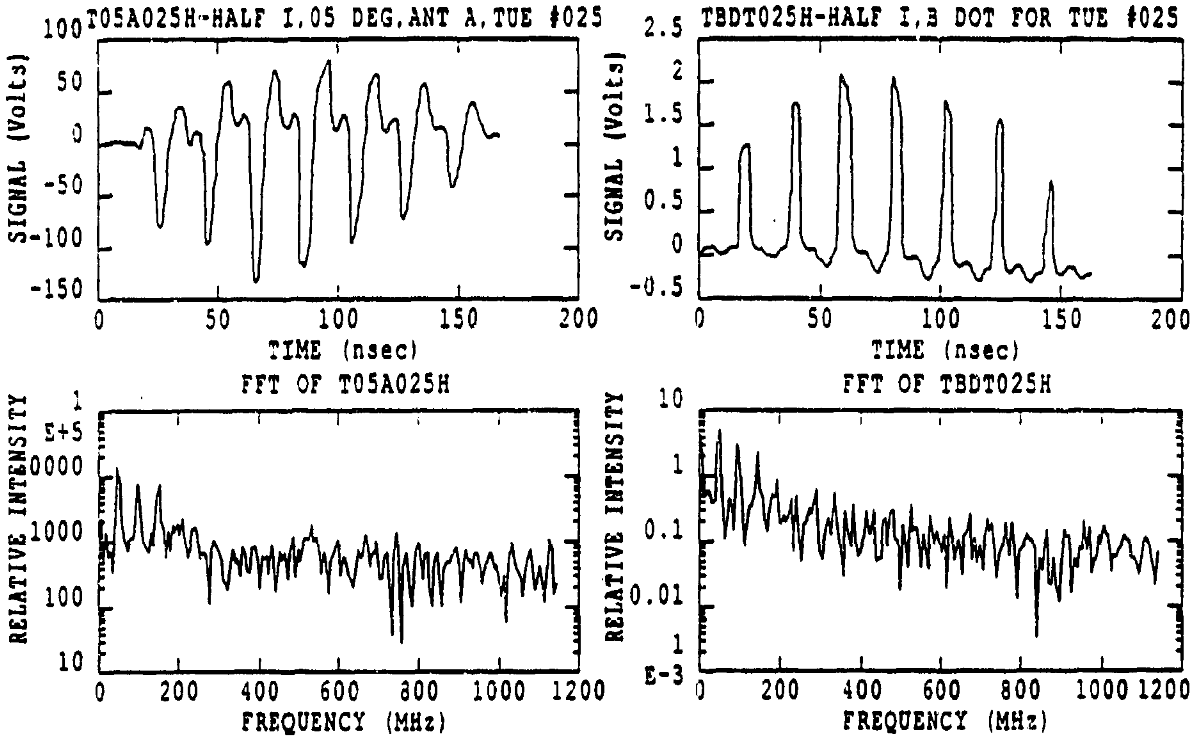

Figure 12. **Example of Program Output**

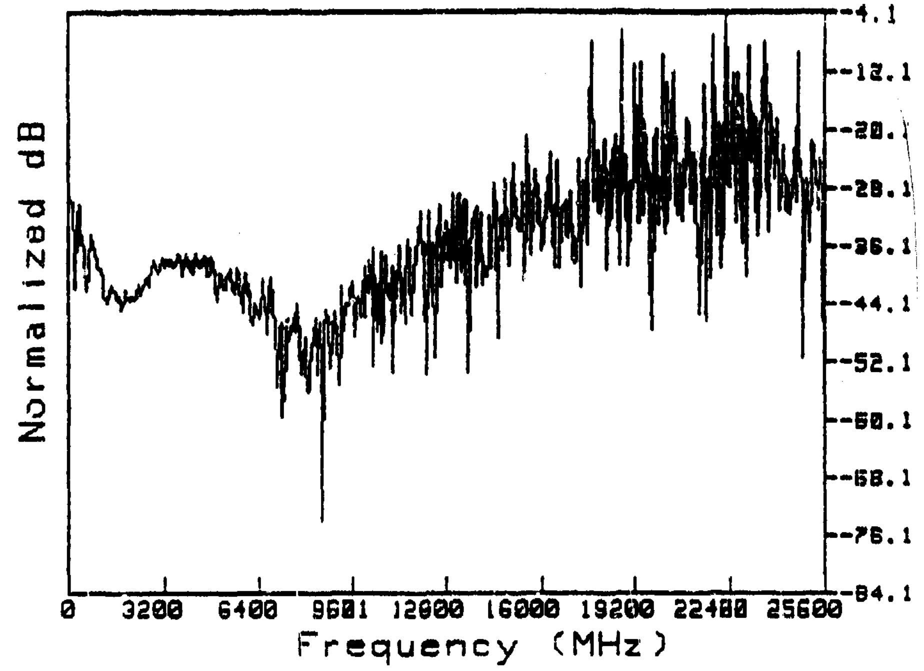

Figure 13. **Antenna Response**

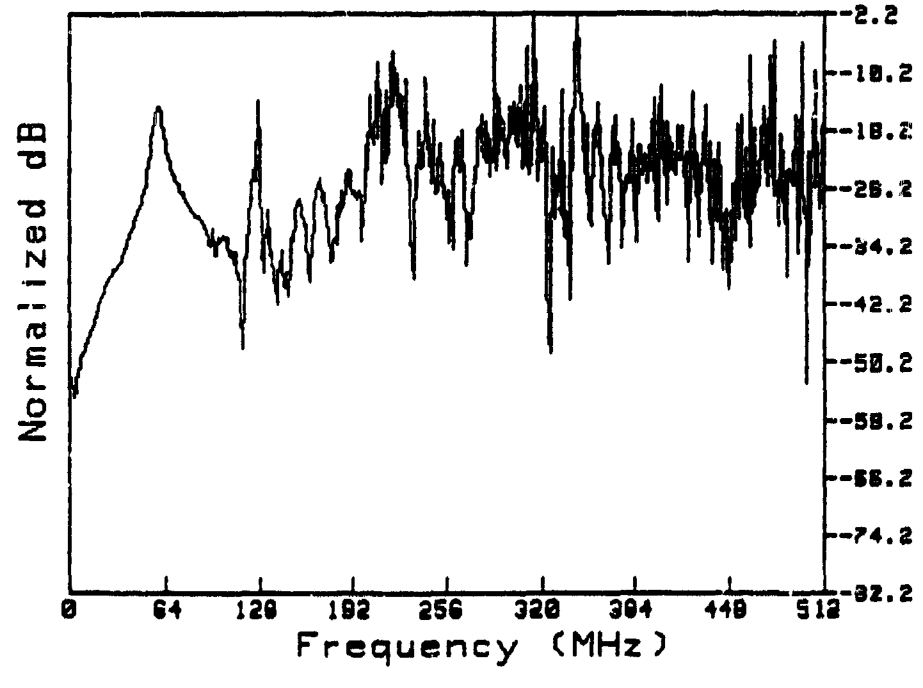

Figure 14. **Antenna Response**

5.3 MHz intervals. This was referred to as the "fine correction." The values provided by the calibration print-out corresponding to Figure 9 were referred to as the "coarse correction."

The correction values are referred to by the NBS National Engineering Laboratory [Ref. 20] as the TEM horn transfer function. The transfer function is defined as

$$TF = 20 \text{ LOG } \frac{V}{E} \qquad (8)$$

where

V = output voltage of TEM horn, rms volts, and

E = electric field strength, volts/meter

The transfer function correction using equation 8 was included in the analysis program to calculate the FFTs. Points lying between the 5 MHz interval in the fine correction case and between 50 MHz interval in the coarse correction case were derived by linear interpolation.

A comparison of the fine correction to the coarse correction is seen in Figure 15. The uncorrected FFT is also plotted to show the effect of the transfer function. The uncorrected FFT displays the characteristic 50 MHz peak and its harmonics. The coarse correction has a similar trace but it was increased in intensity by a factor of about 100. However, the fine correction causes a flattening of the characteristic peaks. This effect is attributed to rapid fluctuations in the graph of responses and to the method of evaluating the closest value. The fine correction had an added disadvantage: it lengthened the program so much that it could not be

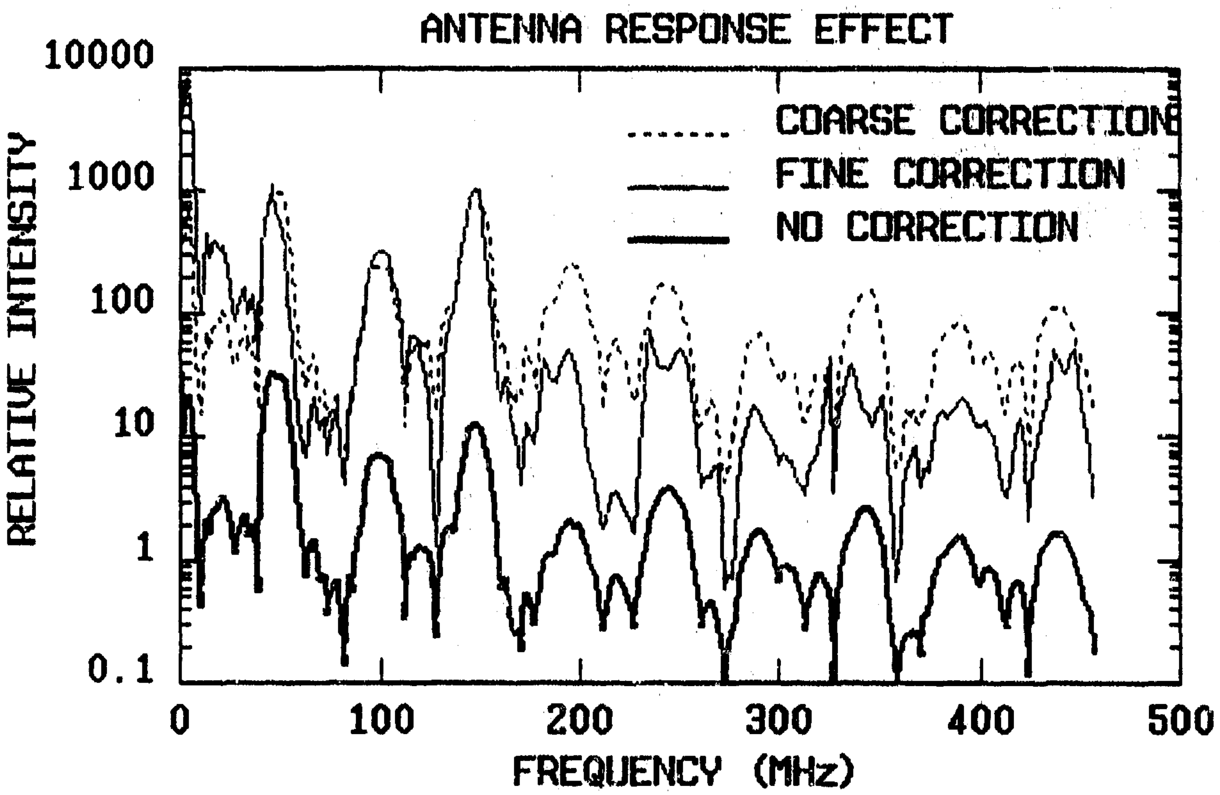

Figure 15. **Comparison of Correction Values**

executed in IDL. The coarse correction was therefore used in evaluating all the FFTs. Figure 16 depicts the transfer function for both antenna A and antenna B1.

Also from the NBS test procedure, the voltage received is related to the electric field E at the antenna, by

$$E = C_f V \tag{9}$$

where $C_f = 96.6$, V is in volts, and E is in volts/m [Ref. 20].

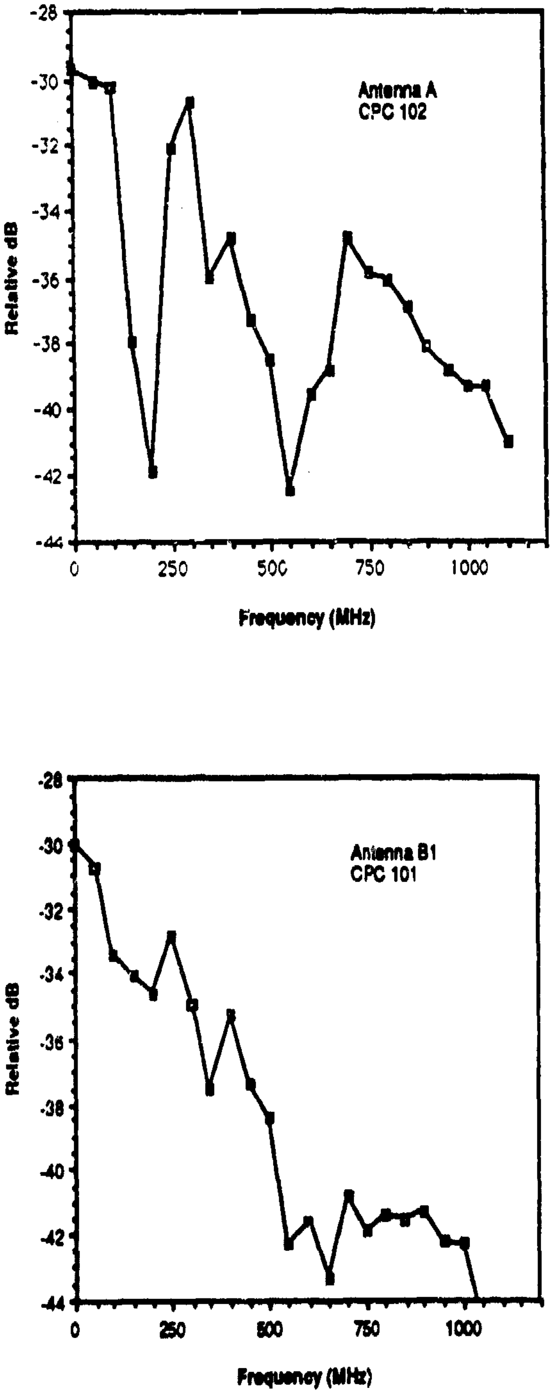

Figure 16. **Antenna A & B1 Transfer Functions**

D. SIGNAL REPRODUCIBILITY

During the experiment, the reproducibility of signals was investigated. A set of three signals obtained at the same angle, under the same beam parameters, and with the same antenna (A) are shown in Figure 17. One immediately notices that the three signals are very similar. However, minor but observable differences in the peaks are apparent. The differences can be attributed to slight changes in the electron beam coupled with an uncalibrated DCS system and slight DC offsets. In general, the recorded signals for each data set are reproducible.

Figure 18 is a set of three signals taken under the same conditions as Figure 17, except that antenna B1 was used. Here, similar effects are seen. Again, the overall conclusion is that the recorded signals are reproducible in each data set.

E. ANTENNA-TO-ANTENNA COMPARISON

As seen in Table 1, antenna A was used primarily at the smaller angles of 5, 10, and 15 degrees. B1 or B2 was normally placed at the larger angles of 30, 45, and 60 degrees. Therefore, a comparison of antenna A to antenna B was required to relate the smaller- and larger-angled values. Figure 19 depicts the signals from antennae A and B1. The beam shot and angular position were exactly the same for both antennae. The signals display similar oscillations and characteristics. However, the maximum peak-to-peak voltage of antenna B1 is approximately one-fifth of antenna A. Antenna B2 was also compared to Antenna A in a similar manner. Table 2 shows the antenna conversions for B1 and B2 to antenna A.

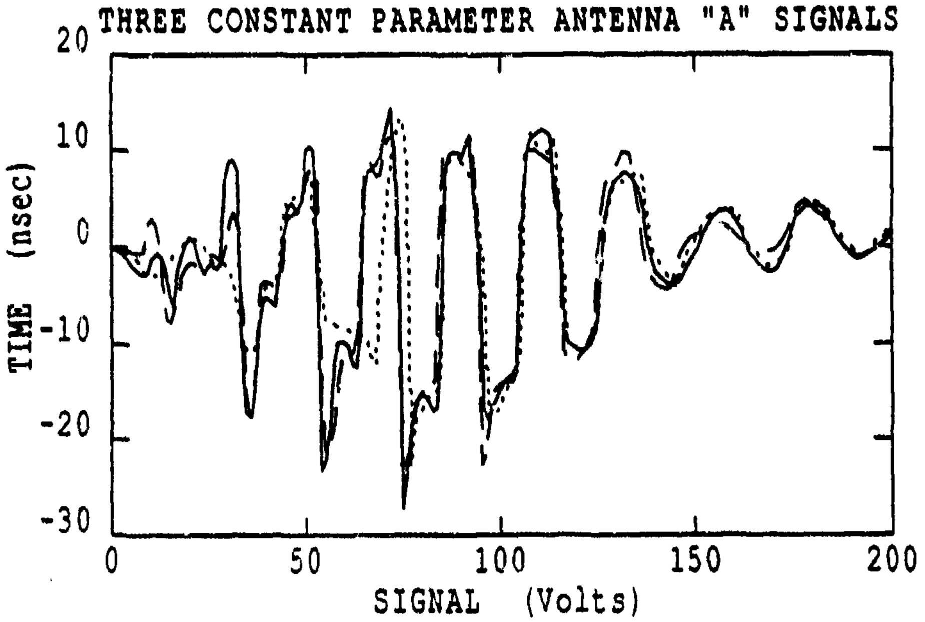

Figure 17. **Reproducible Signals from Antenna A**

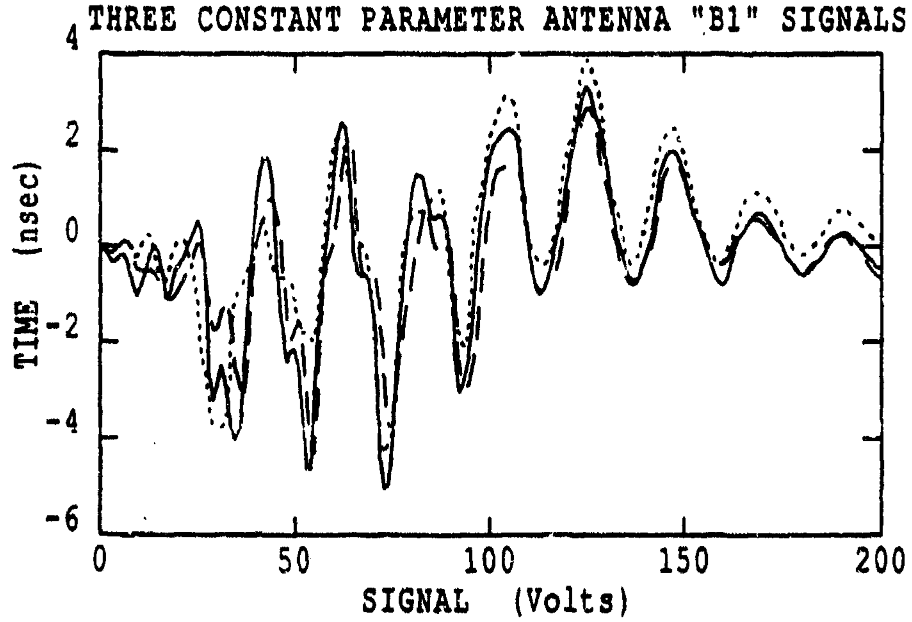

Figure 18. **Reproducible Signals from Antenna B1**

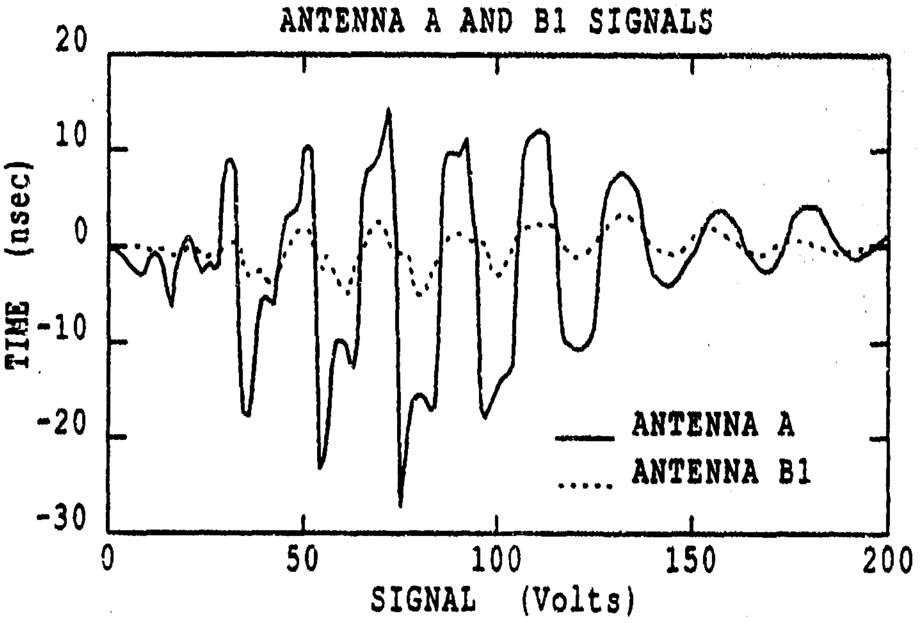

Figure 19. **Comparison of Antenna A and B1 Signals**

TABLE 2

ANTENNA CONVERSION

Antenna	**Factor to Convert Antenna B Signal to Antenna A**
CPC 101 (Antenna B1)	4.9
CPC 102 (Antenna A)	1.0
CPC 103 (Antenna B2)	0.33

It was found that antenna B1 compared much more favorably than antenna B2 to antenna A. The signals from antenna B2 were very sharp and appeared almost erratic. Antennae A and B1 signals were much smoother. However, as mentioned in the previous section, the signals were reproducible for each data set recorded with the same antenna.

IV. RESULTS AND DISCUSSION

A. RESULTS

The experimental results are organized into five areas: signals and related spectrum, signal strength as a function of angle, relative intensity of spectrum harmonics, shifting of fundamental frequency, and modulation of spectrum. A discussion of the following results appears in the next section.

1. Signals and Related Spectrum

A complete set of all radiation and B dot signals along with their respective spectra was created using the IDL program. However, here one signal per angle (5, 10, 15, 30, 45, and 60 degrees) and beam parameter are provided for completeness. Figure 20–22, Figures 23–25, Figures 26–28, and Figures 29–31 are signal and B dot results for full current, half current, diffuse beam (full current), and half energy beam (half current), respectively.

2. Signal Strength as a Function of Angle

For each radiation signal from each data set, the maximum peak-to-peak voltage was measured. This value divided by two was also converted into the actual electric field strength using equation 9. The current for each beam shot was computed using equation 7 and tabulated in Table 3. Difficulties with the B dots on the first day caused inaccurate current readings. It is assumed that the current was

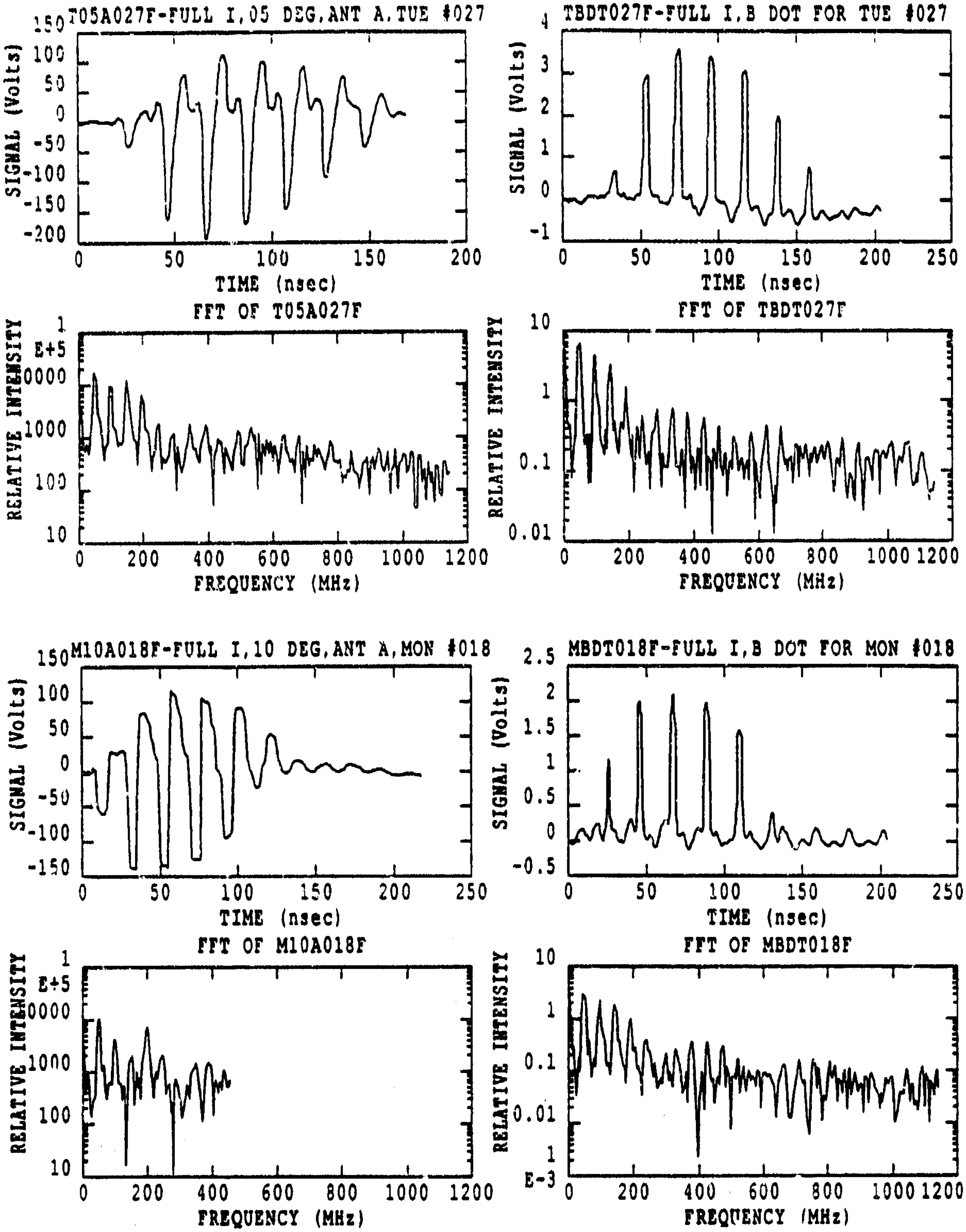

Figure 20. **Signal and Spectrum for Full Current, Full Energy, Angles of 5 and 10 Degrees**

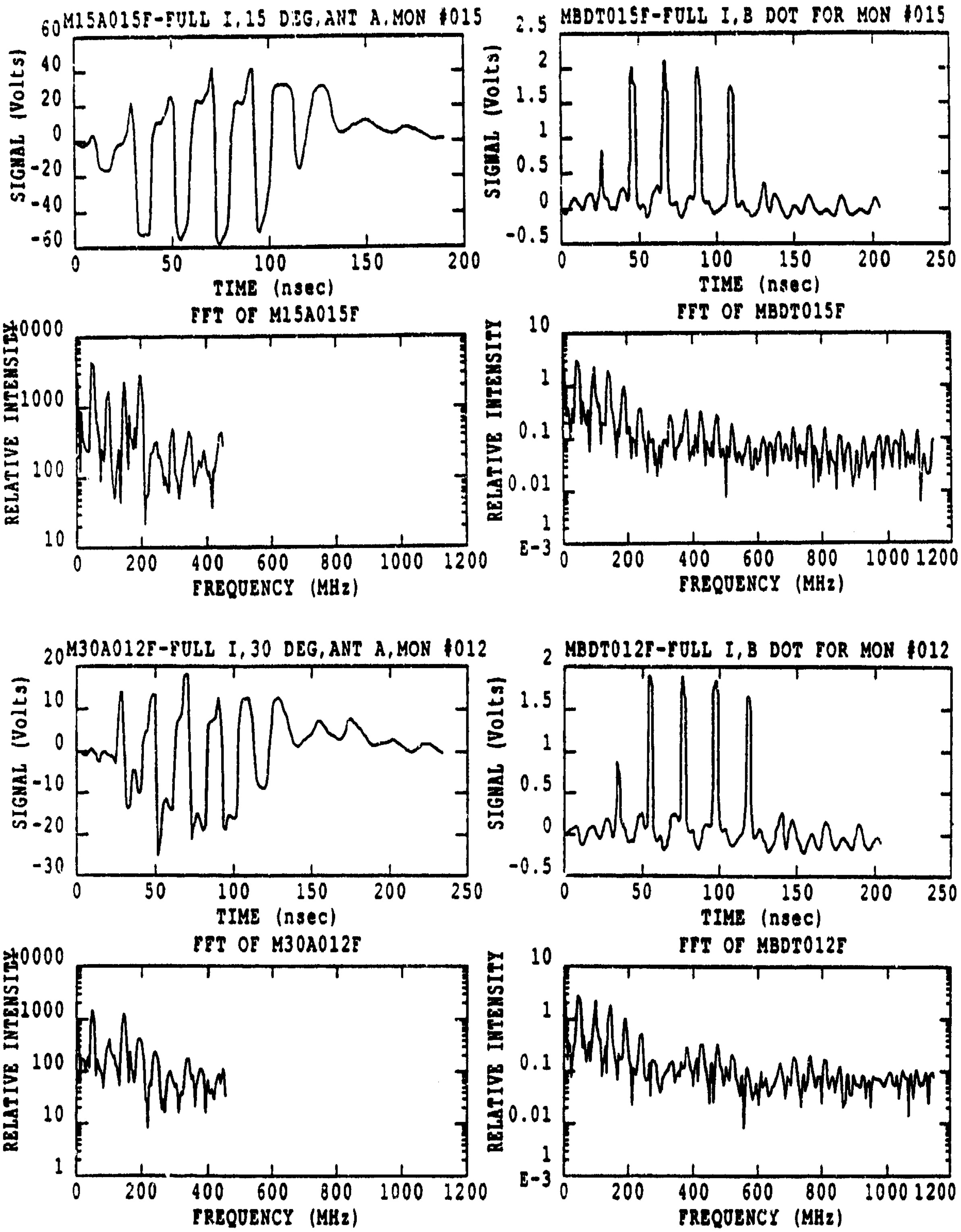

Figure 21. **Signal and Spectrum for Full Current, Full Energy, Angles of 15 and 30 Degrees**

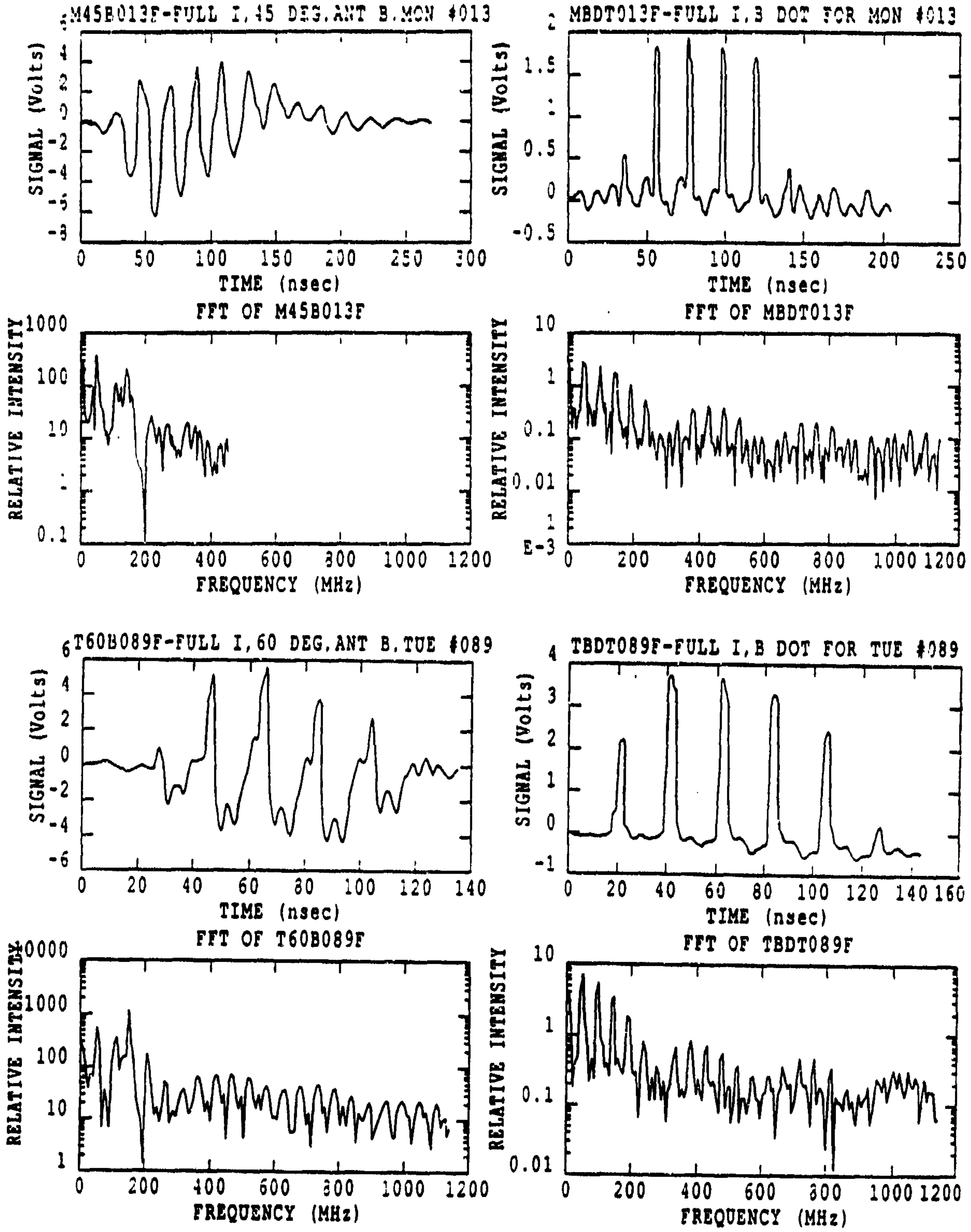

Figure 22. **Signal and Spectrum for Full Current, Full Energy, Angles of 45 and 60 Degrees**

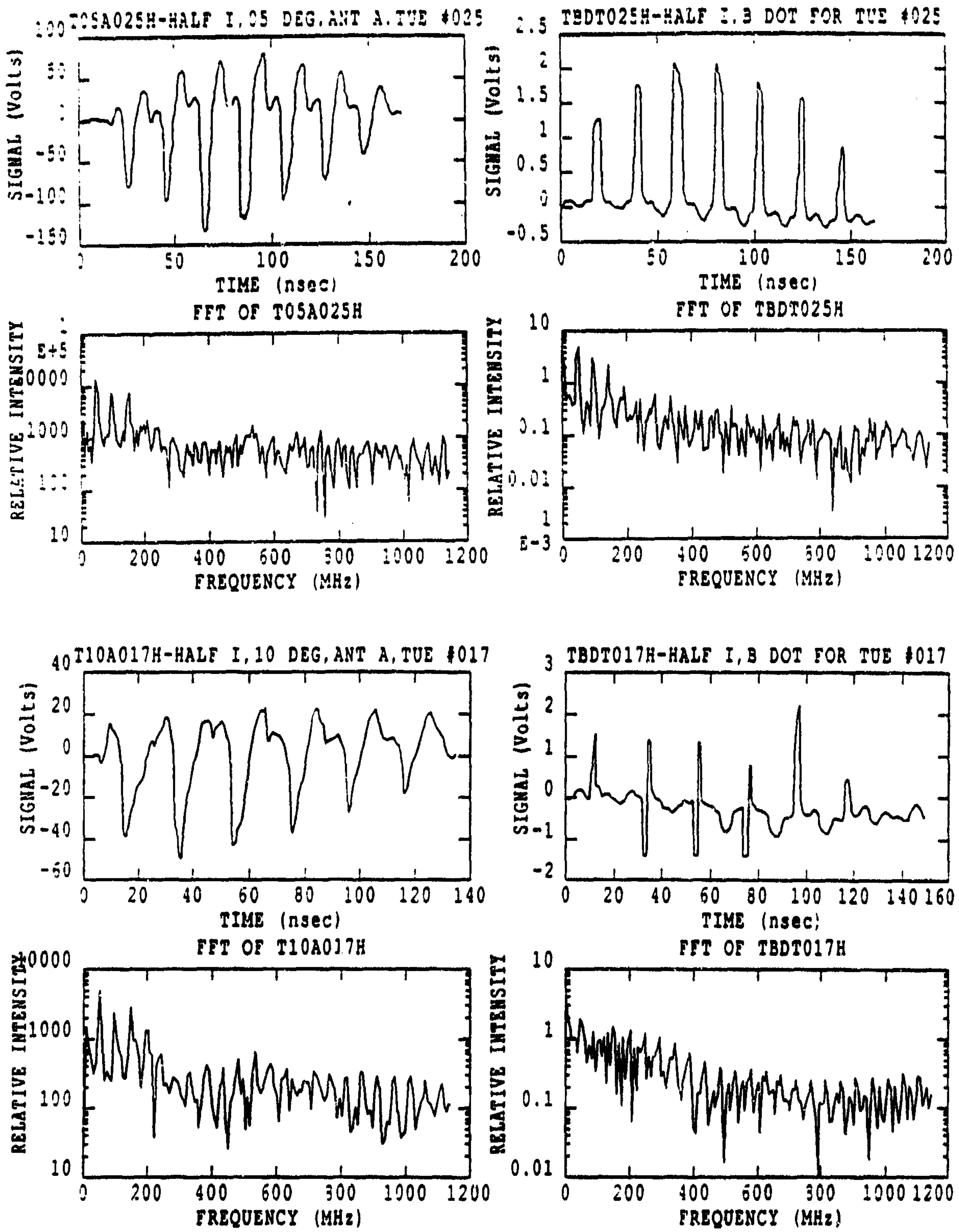

Figure 23. **Signal and Spectrum for Half Current, Full Energy, Angles of 5 and 10 Degrees**

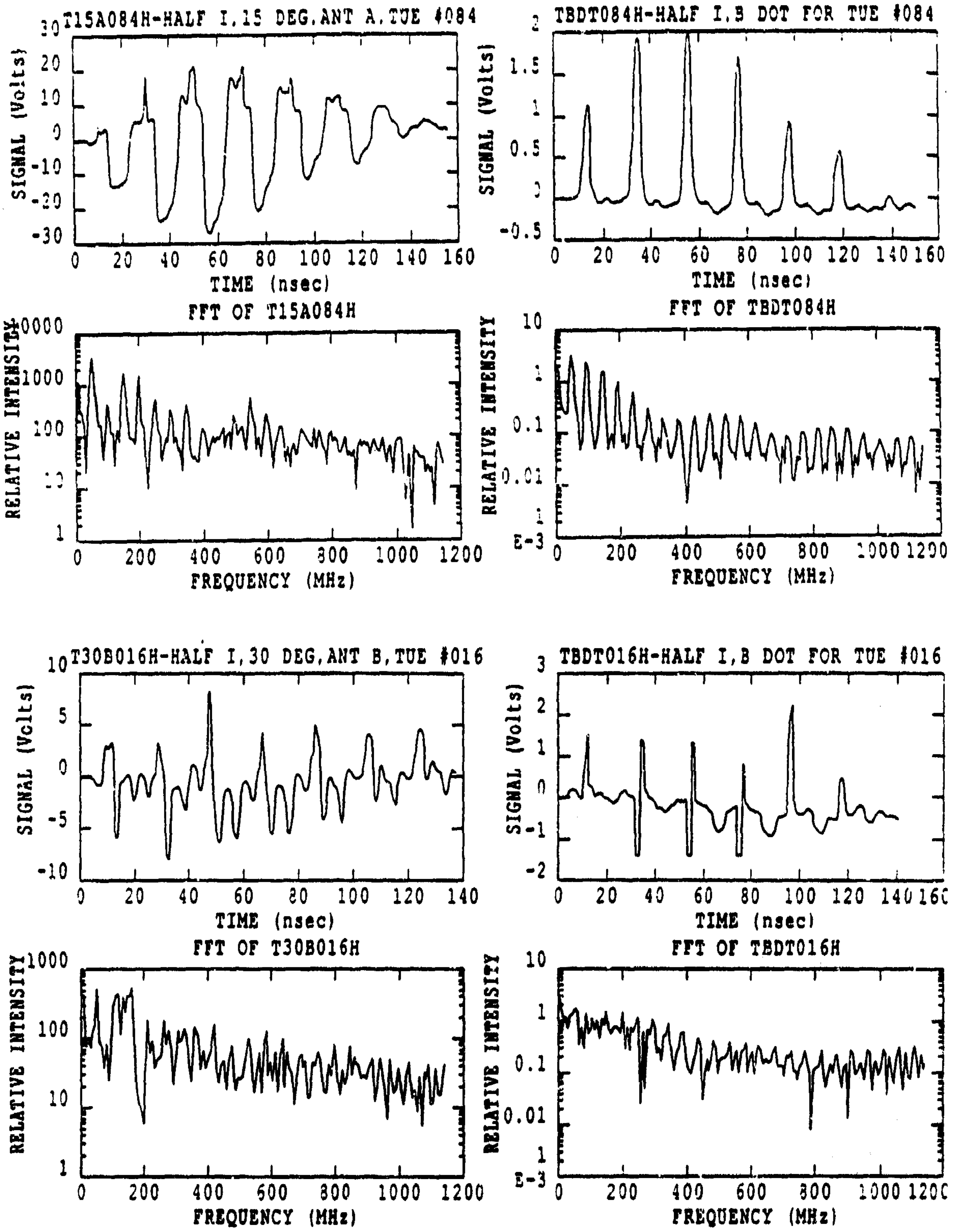

Figure 24. **Signal and Spectrum for Half Current, Full Energy, Angles of 15 and 30 Degrees**

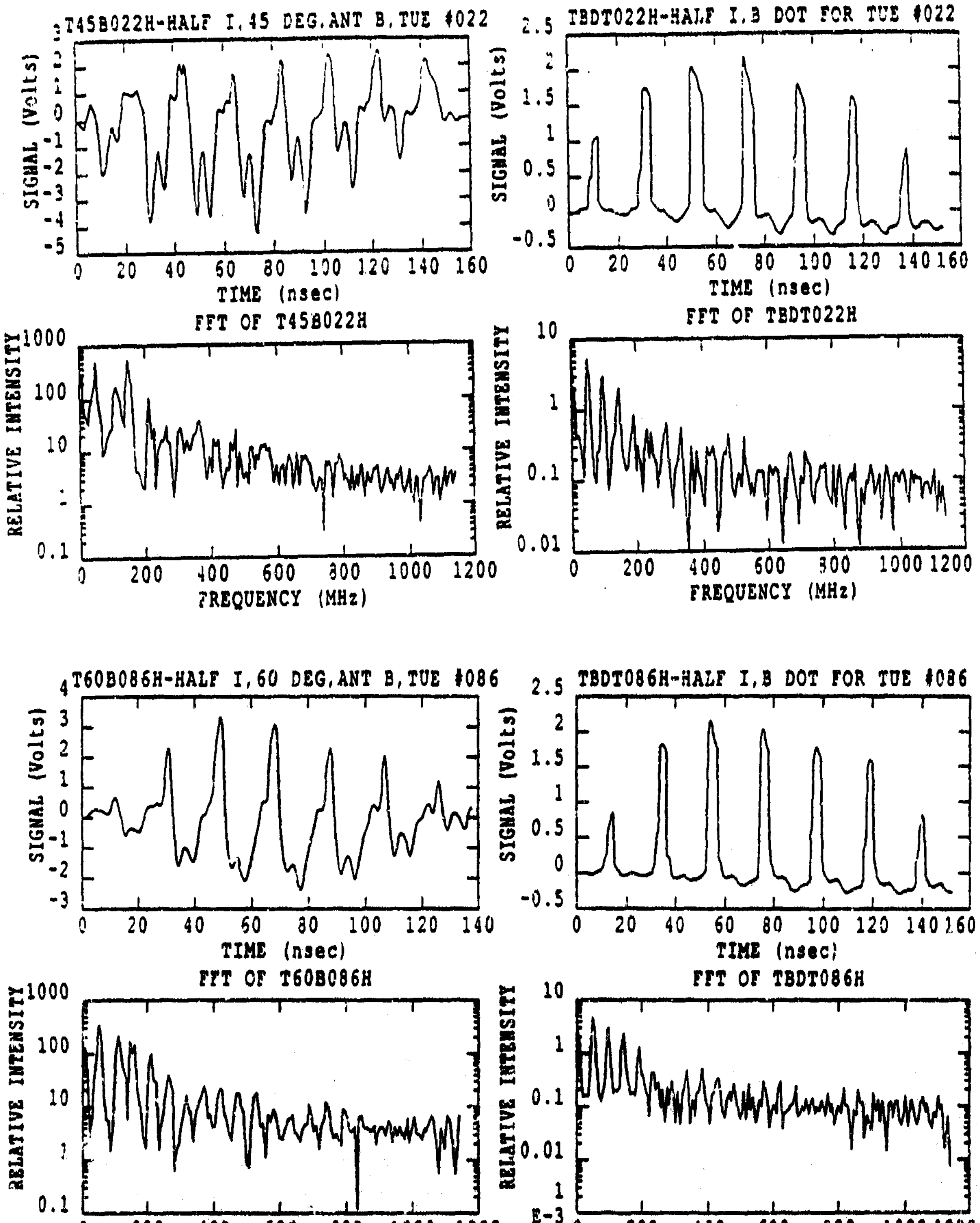

Figure 25. **Signal and Spectrum for Half Current, Full Energy, Angles of 45 and 60 Degrees**

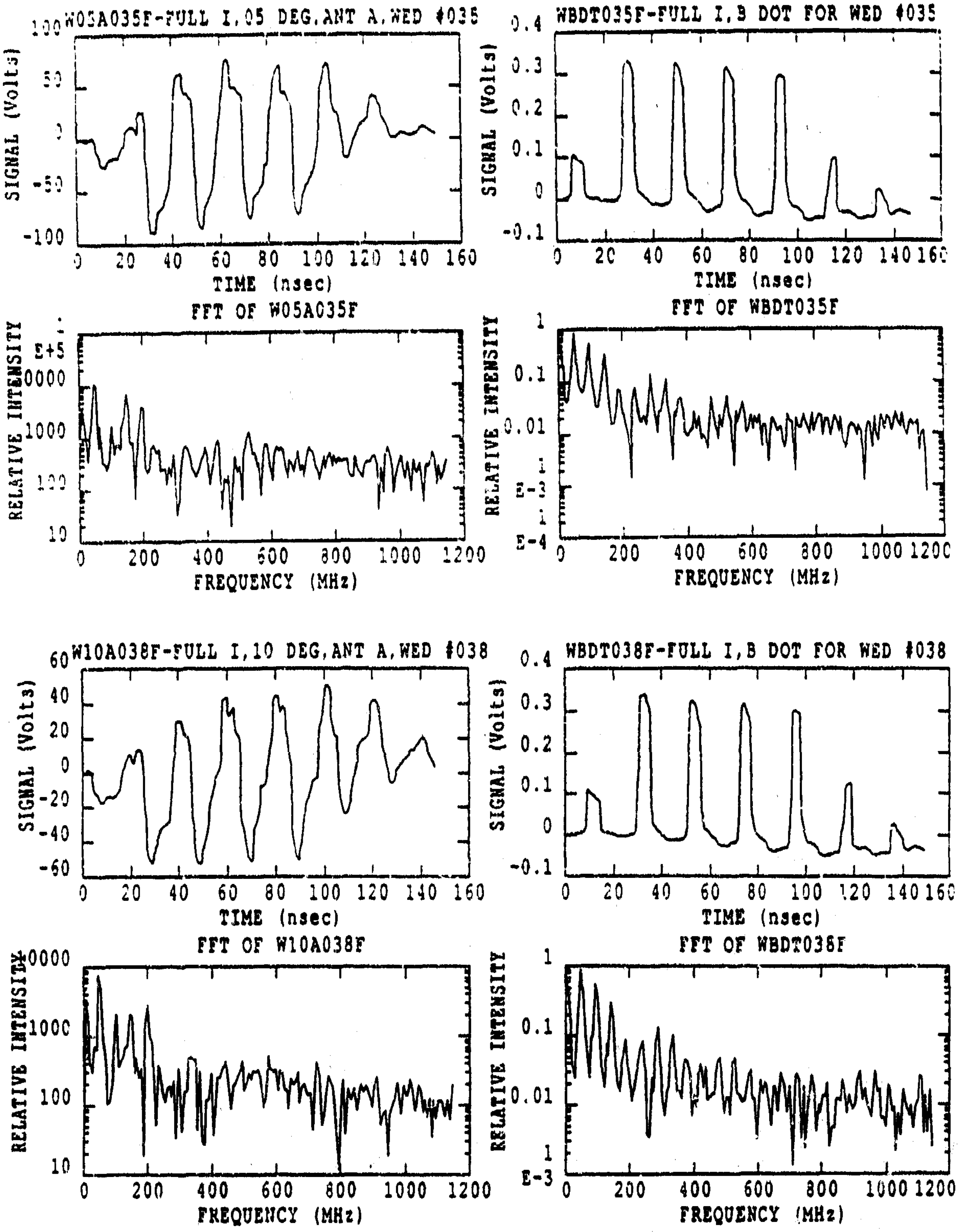

Figure 26. **Signal and Spectrum for Diffuse Beam, Full Current, Full Energy, Angles of 5 and 10 Degrees**

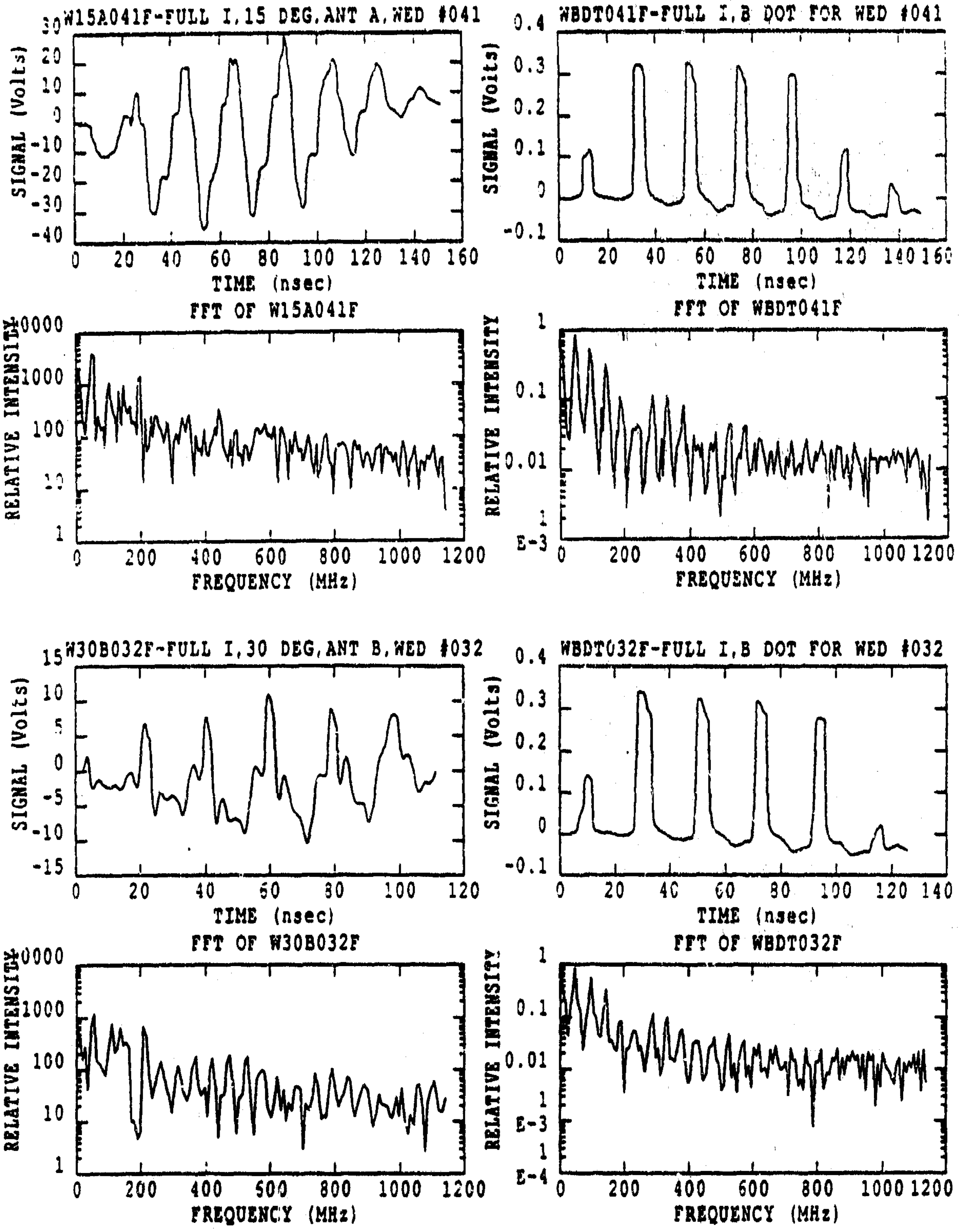

Figure 27. **Signal and Spectrum for Diffuse Beam, Full Current, Full Energy, Angles of 15 and 30 Degrees**

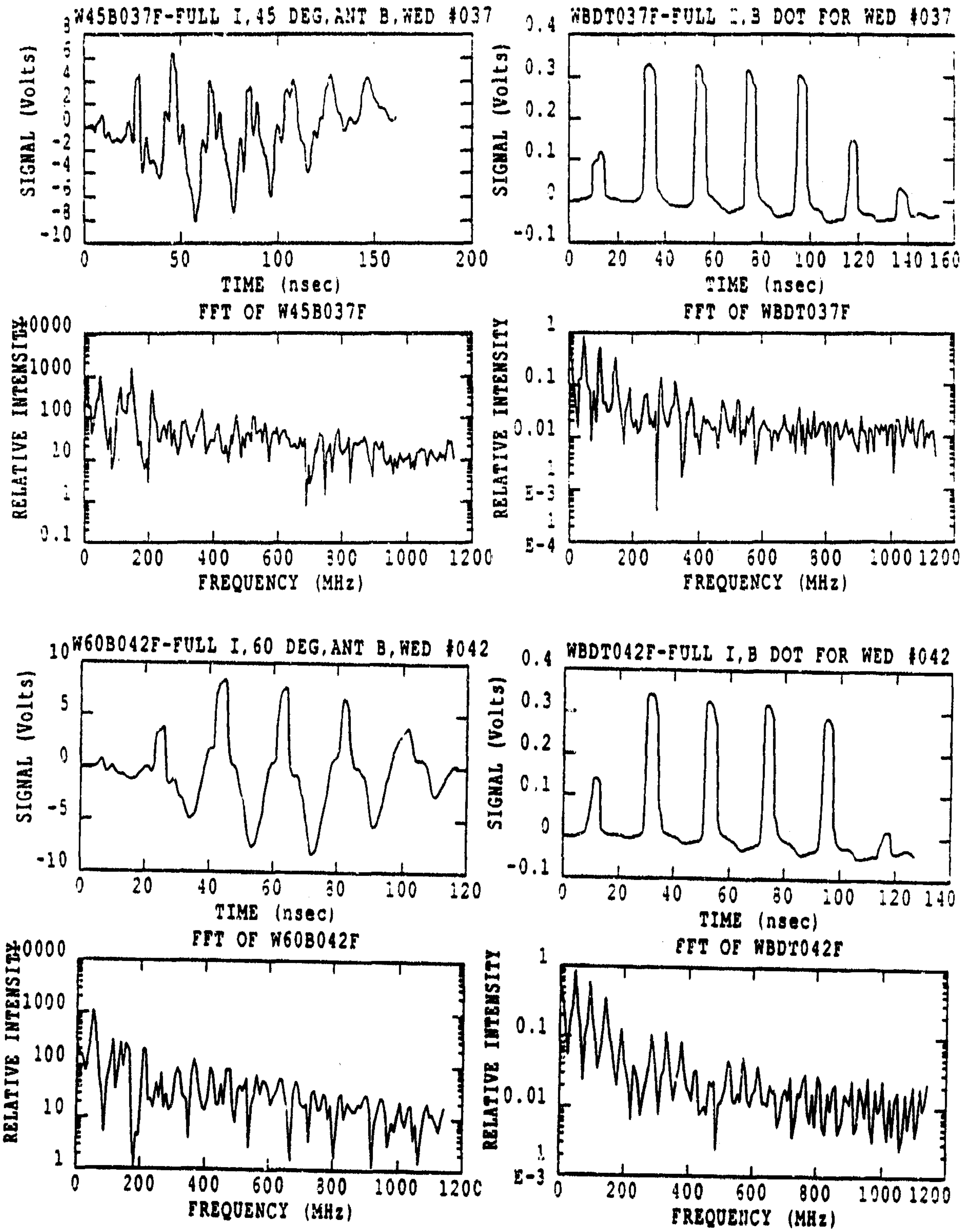

Figure 28. **Signal and Spectrum for Diffuse Beam, Full Current, Full Energy, Angles of 45 and 60 Degrees**

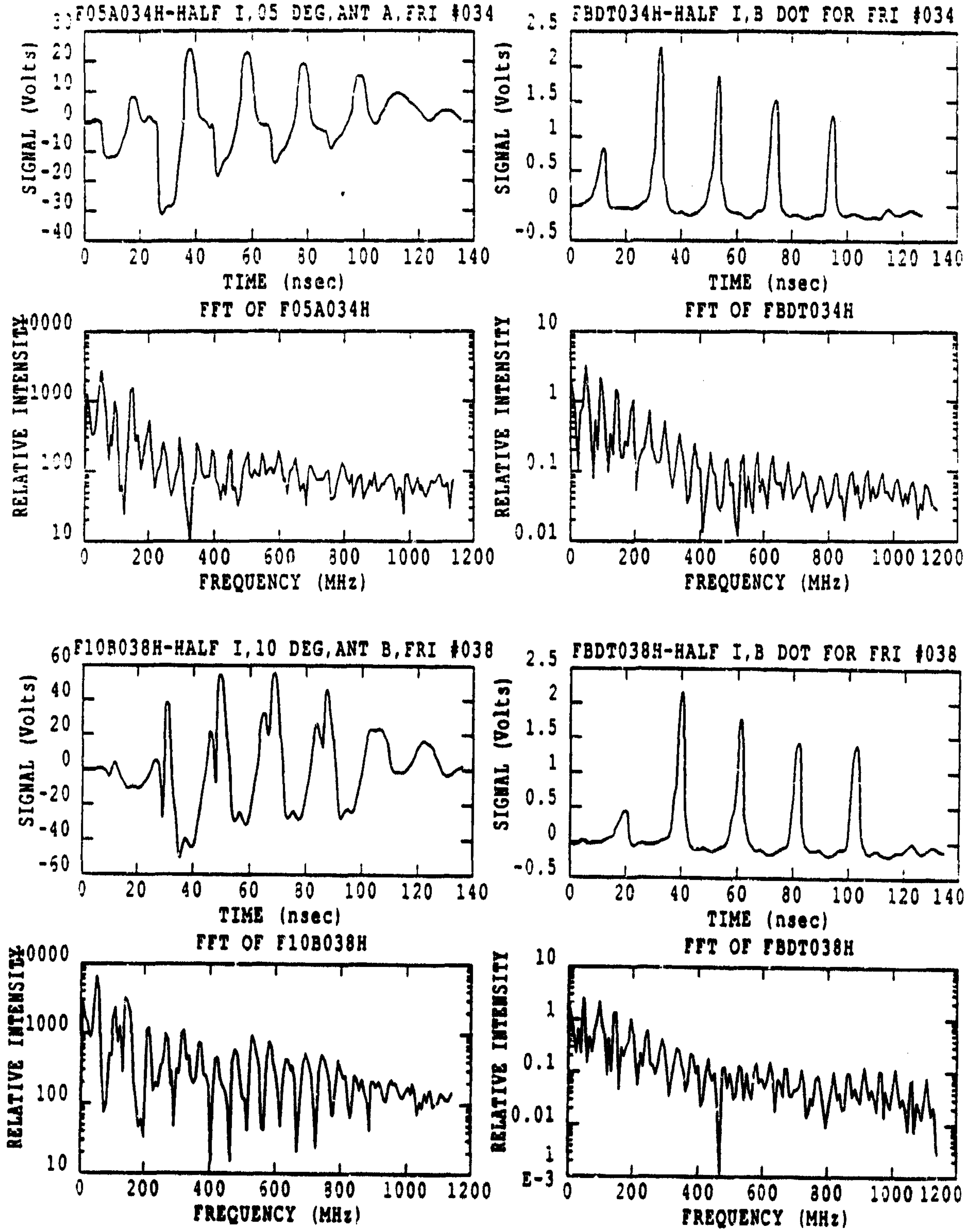

Figure 29. **Signal and Spectrum for Half Energy, Half Current, Angles of 5 and 10 Degrees**

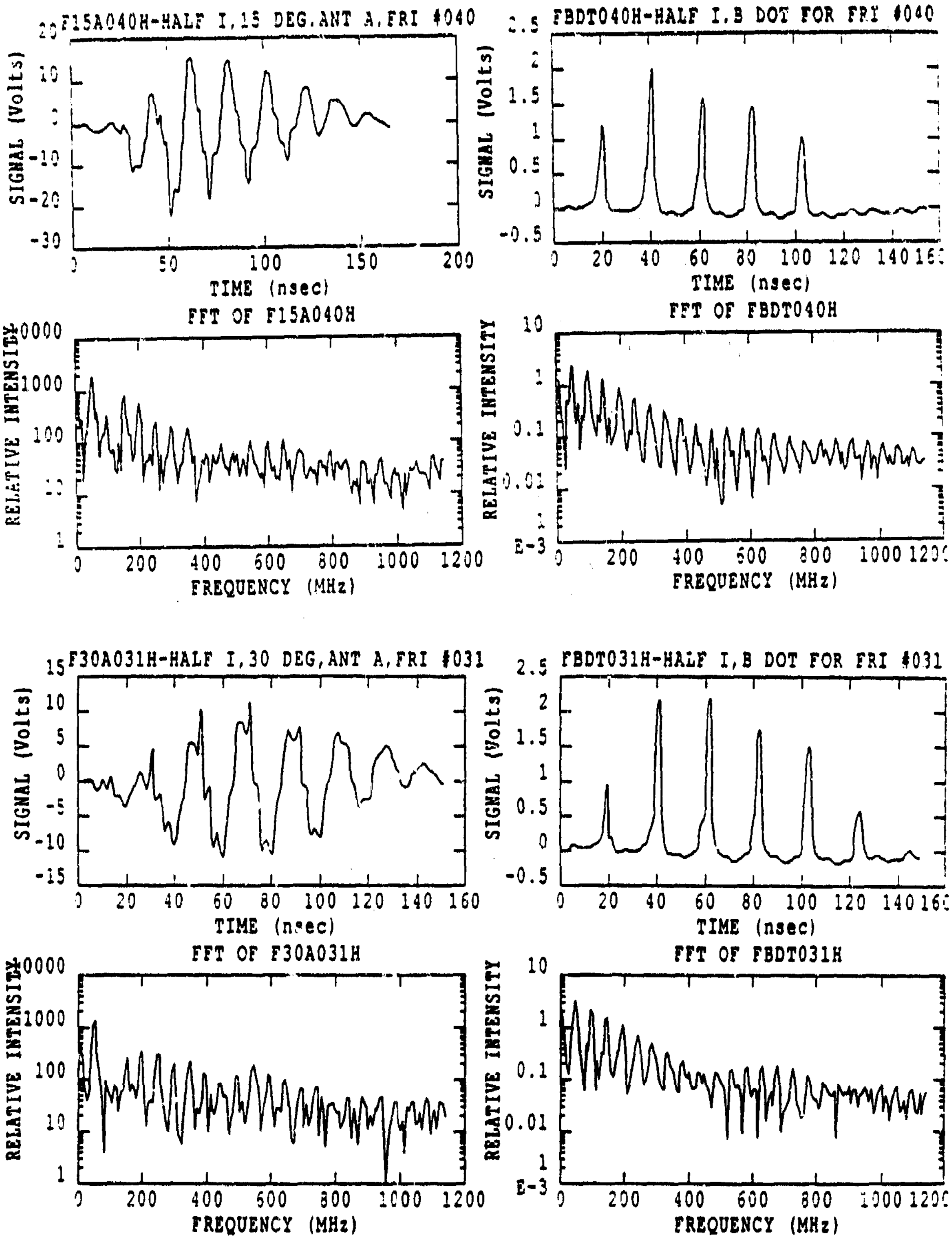

Figure 30. **Signal and Spectrum for Half Energy, Half Current, Angles of 15 and 30 Degrees**

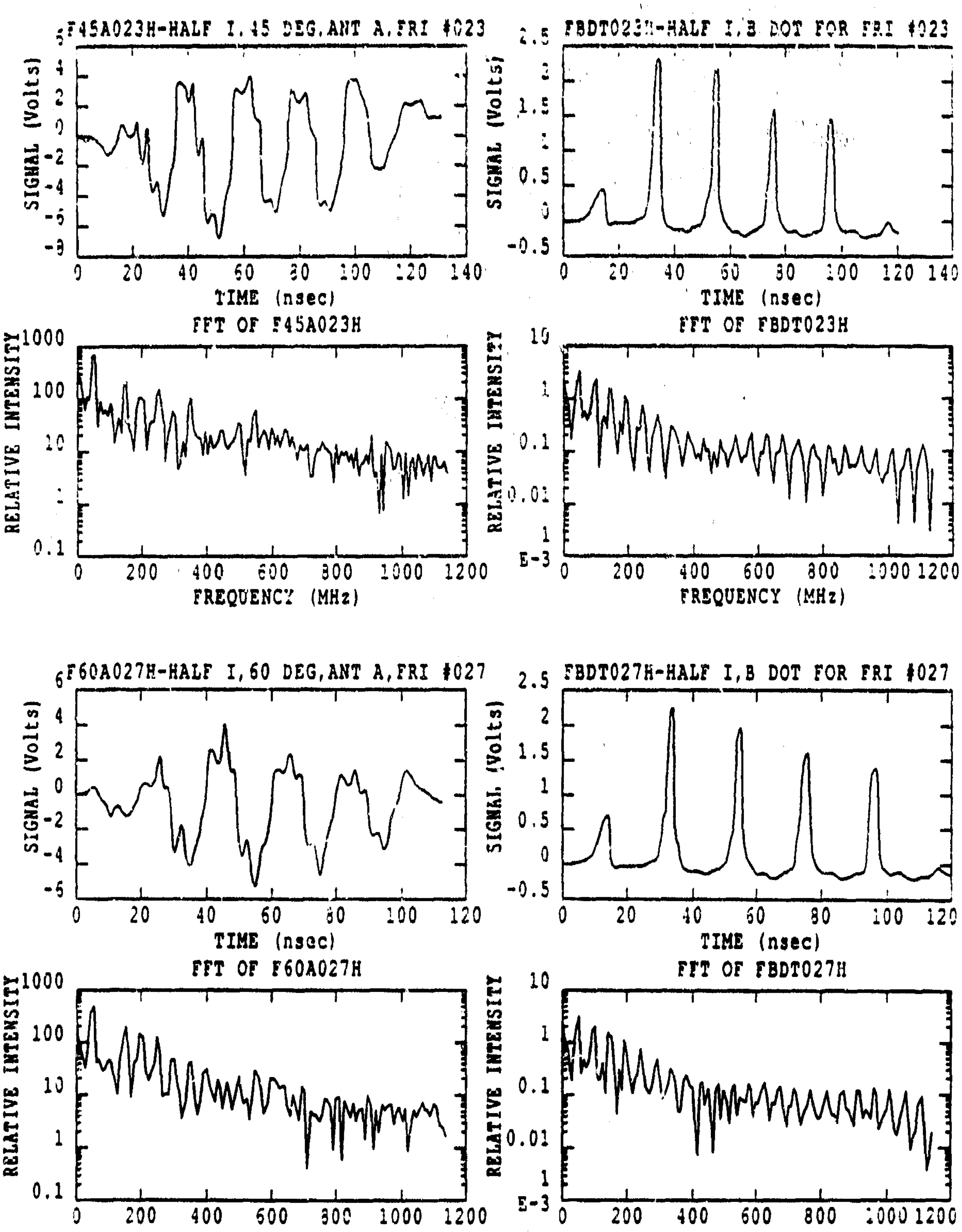

Figure 31. **Signal and Spectrum for Half Energy, Half Current, Angles of 45 and 60 Degrees**

TABLE 3

ACTUAL BEAM CURRENTS (IN AMPS)

Beam Parameter	Angles in Degrees					
	5	10	15	30	45	60
Full Current	495 ± 13	286 ± 12*	275 ± 14*	263 ± 5*	270 ± 2*	328 ± 9
Half Current	302 ± 15	404 ± 2	297 ± 2	265 ± 5	310 ± 7	292 ± 13
Diffuse	463 ± 22	449 ± 5	456 ± 5	463 ± 22	449 ± 5	456 ± 5
Half Energy	312 ± 2	288 ± 13	288 ± 13	303 ± 20	319 ± 1	303 ± 7

*Problems with B dot registered in accurate currents. Actual currents were approximately 500 amps.

approximately 500 A for that day (for full-current tight beam). Since the current, angle, and distance are all known values, the expected electric field can be determined using equation 6. A comparison of expected to actual electric fields is in Table 4. The average radiation peak-to-peak value was also plotted as a function of angle. Full versus half current (Figure 32), tight versus diffuse beam (Figure 33), and full versus half current (Figure 34) were compared. In addition, the ratio of the upper curve to the lower curve for the plotted points was compared. The ratio of curves for full versus half current, tight versus diffuse beam, and full versus half energy are exhibited in Figures 35, 36, and 37, respectively.

3. Relative Intensity of Spectrum Harmonics

The fundamental frequency and harmonics are easily observed in the spectrum. By using the interactive version of the IDL program, the

TABLE 4

COMPARISON OF ACTUAL TO EXPECTED ELECTRIC FIELD

	Degrees	**5**	**10**	**15**	**30**	**45**	**60**
Full Current	Actual $\left(\times 10^3 \frac{v}{m}\right)$	14.4 ± .7	12 ± 1	4.9 ± .6	2.0 ± .3	2.12 ± .06	2.3 ± .1
	Expected $\left(\times 10^3 \frac{v}{m}\right)$	9.85 ± .09	6.4 ± .1	4.2 ± .1	2.08 ± .02	1.35 ± .01	1.00 ± .01
Half Current	Actual $\left(\times 10^3 \frac{v}{m}\right)$	9.85 ± .09	3.3 ± .1	2.6 ± .1	3.3 ± .4	1.5 ± .1	1.32 ± .05
	Expected $\left(\times 10^3 \frac{v}{m}\right)$	7.5 ± .4	5.04 ± .02	2.46 ± .02	1.27 ± .03	.82 ± .02	.56 ± .03

relative intensity for each harmonic J was then plotted versus angle. This was repeated for the first four higher harmonics (Figures 38–41) for the four different beam parameters. However, the full current was carried out to the ninth harmonic (see Figure 42).

4. Harmonic Frequency Shift

Again, by using the interactive version of the IDL program, the frequency of each harmonic was evaluated. The average harmonic for each shot was calculated by plotting the frequency against the harmonic number J. A least square fit of the points provided the slope or the overall average frequency. The slopes for shots at the same angle and beam parameters were averaged. This average frequency (approximately 50 MHz) was then plotted versus angle for both full (Figure 43) and half

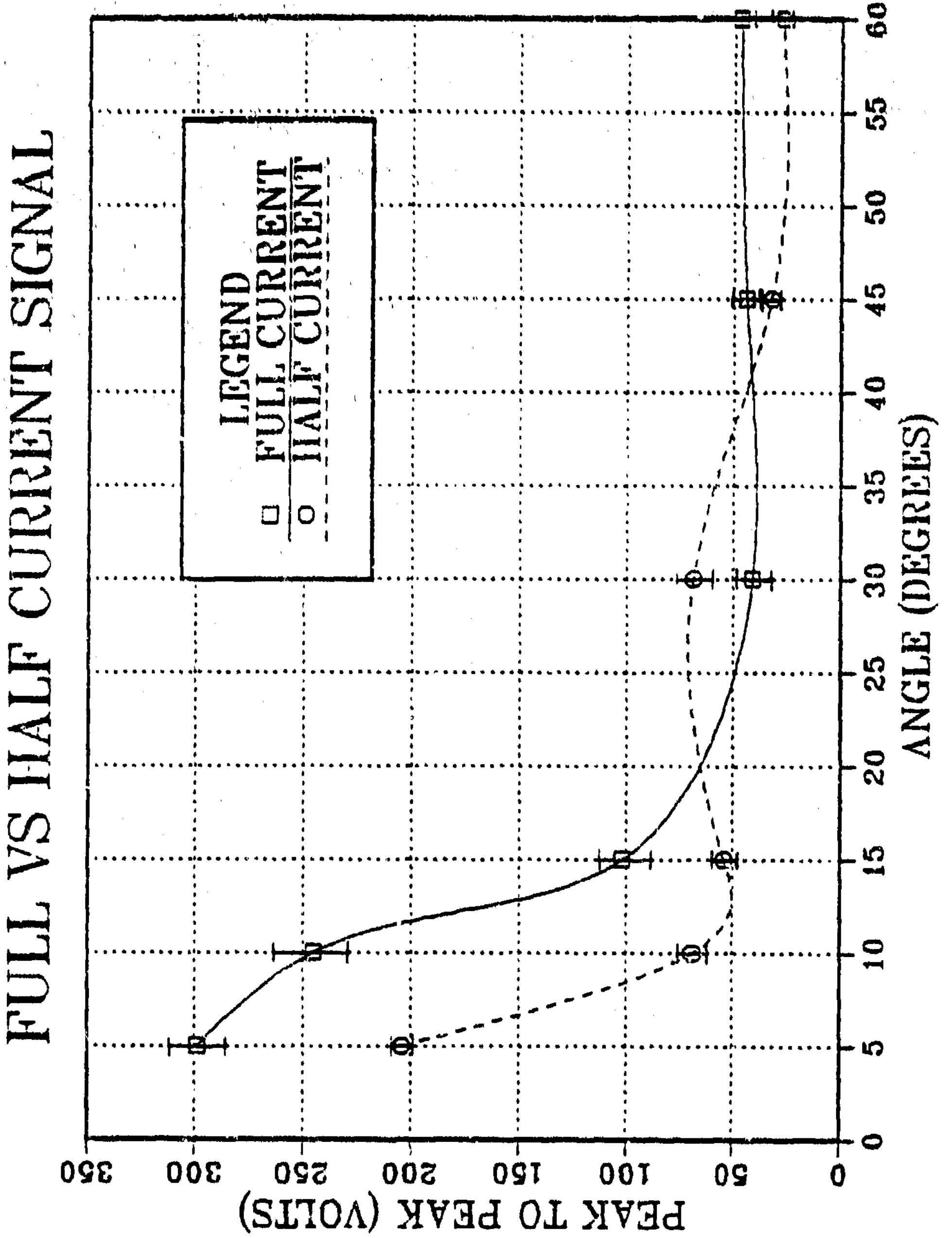

Figure 32. **Signal Strength of Full Versus Half Current (Full Energy)**

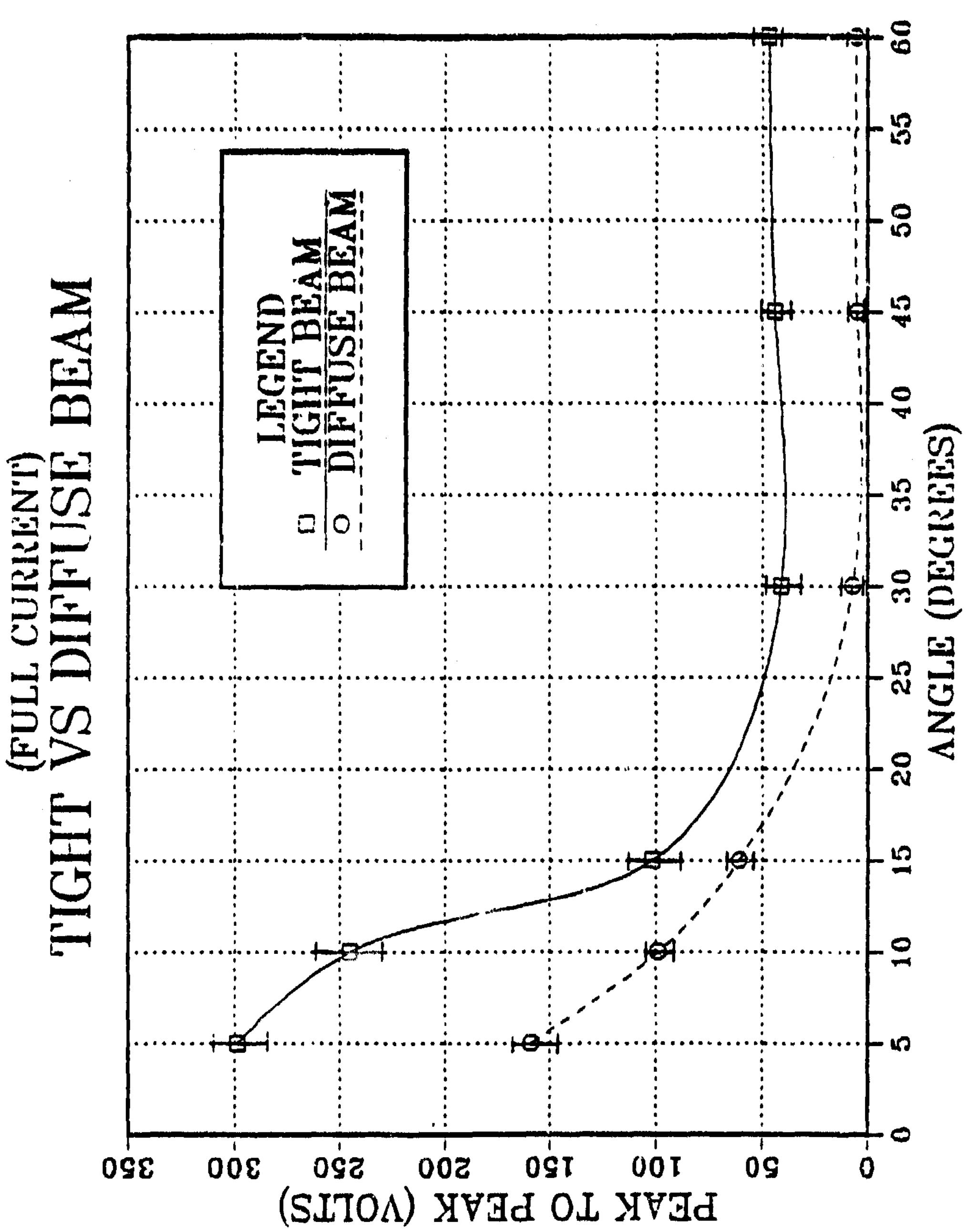

Figure 33. **Signal Strength of Tight Versus Diffuse Beam (Full Current, Full Energy)**

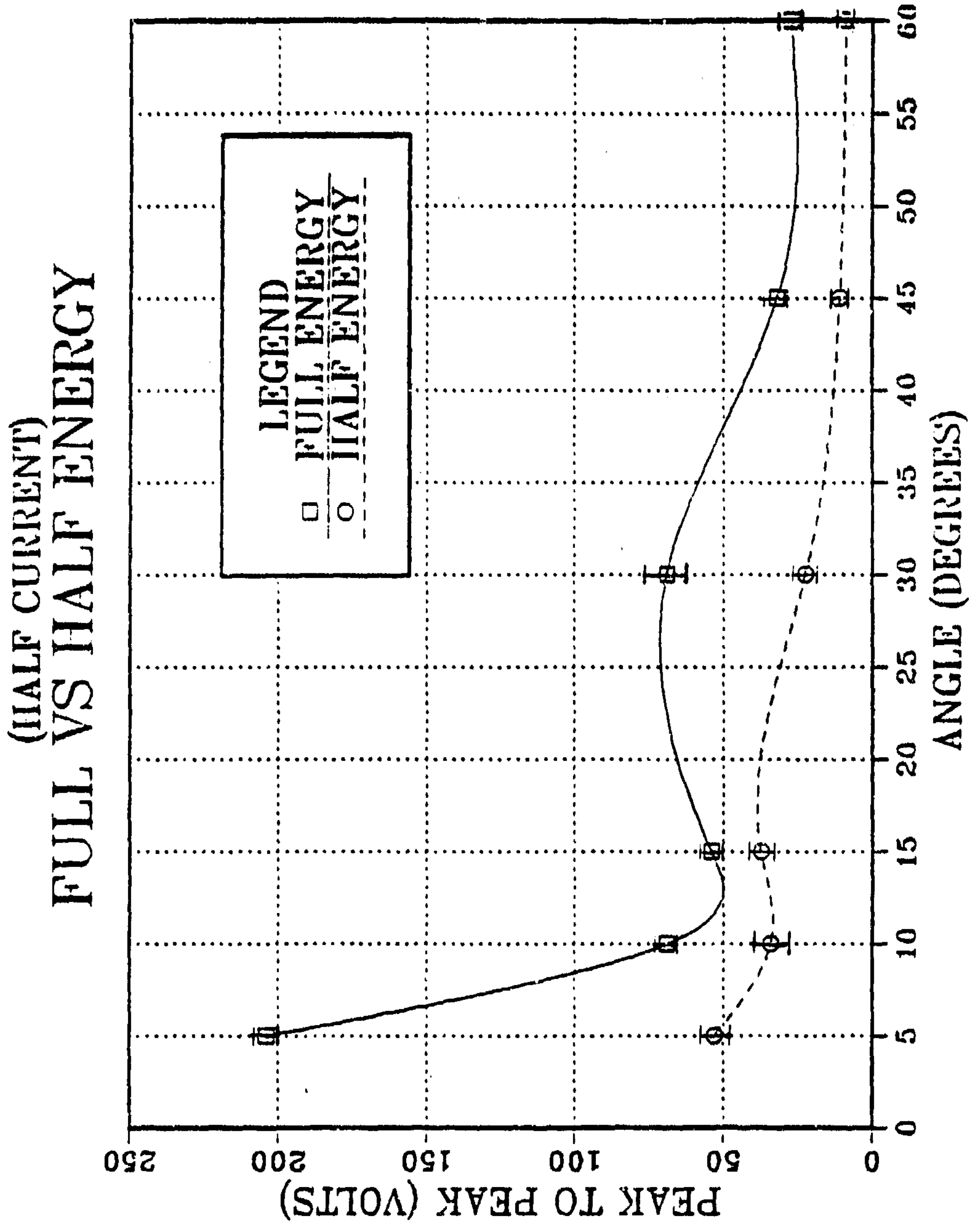

Figure 34. **Signal Strength of Full Versus Half Energy (Half Current)**

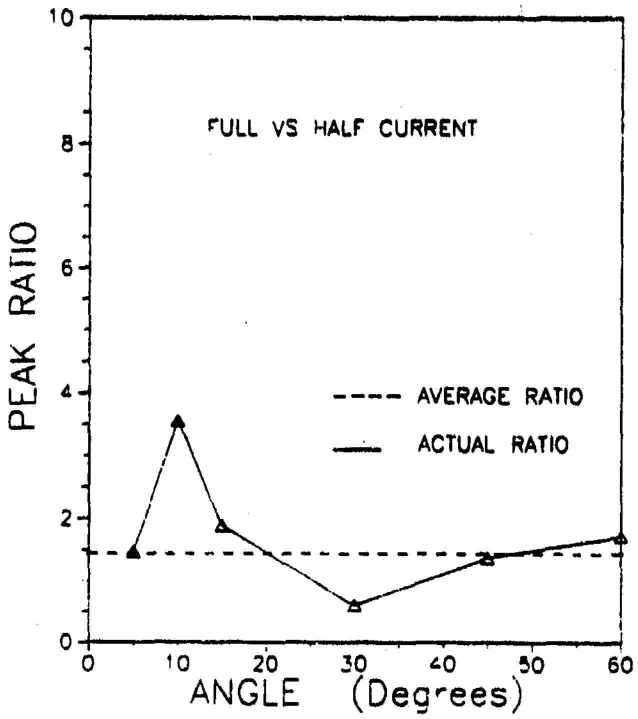

Figure 35. **Ratio of Full to Half Current Signals**

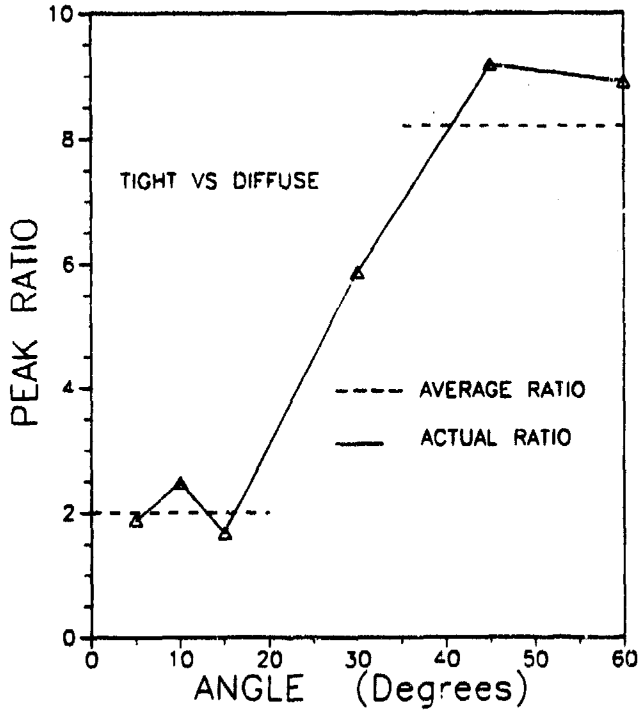

Figure 36. **Ratio of Tight to Diffuse Beam Signals**

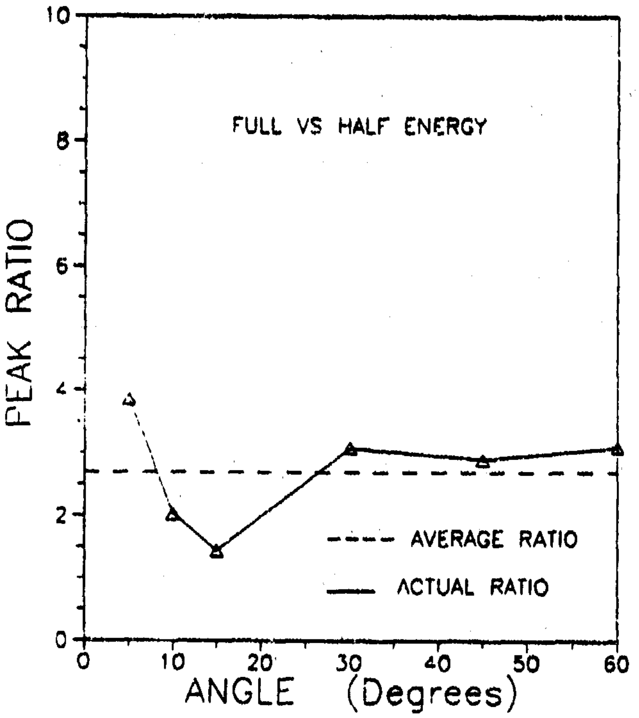

Figure 37. **Ratio of Full to Half Energy Beam Signals**

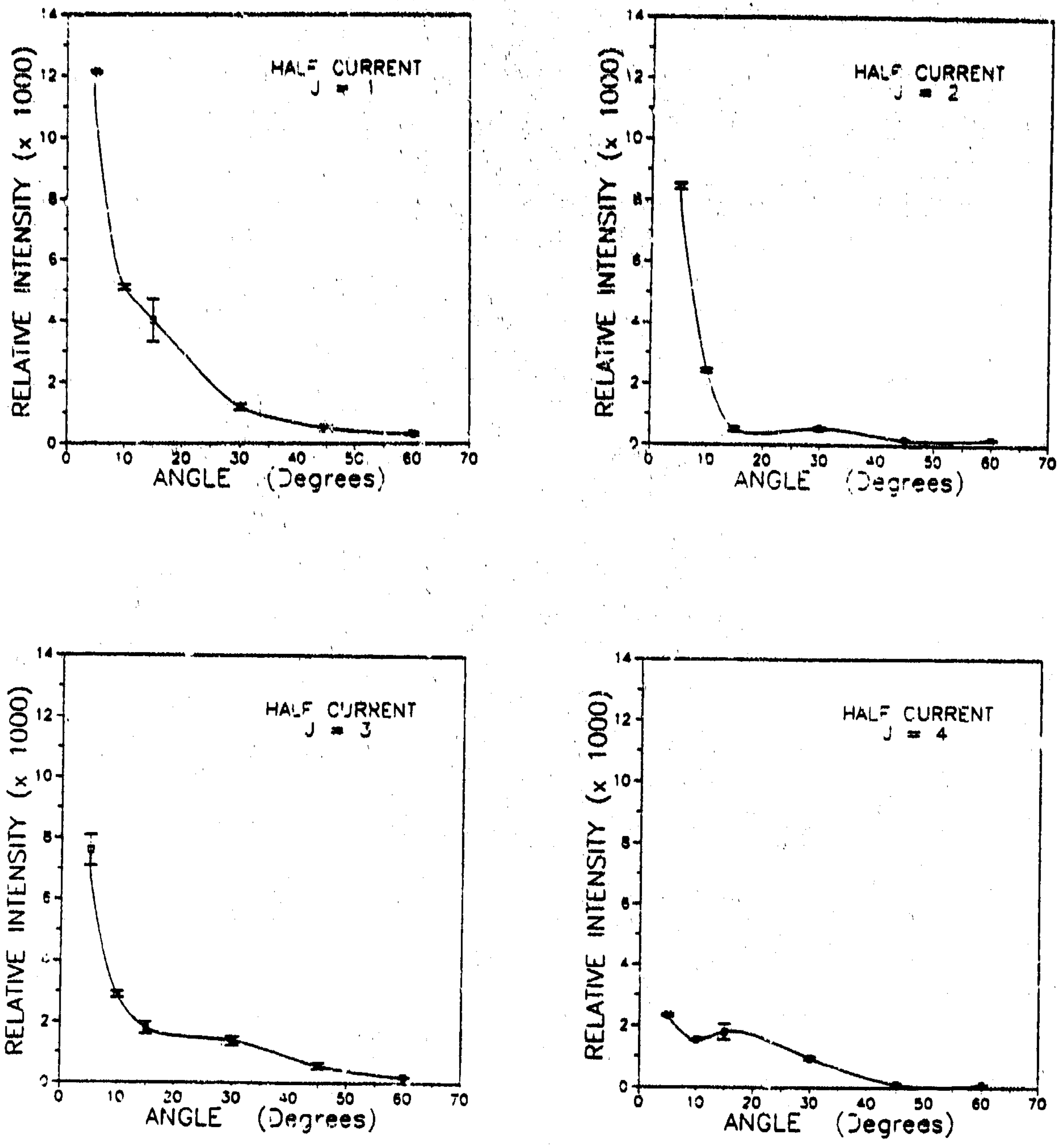

Figure 38. **First Four Harmonics of Half Current Spectrum (Full Energy)**

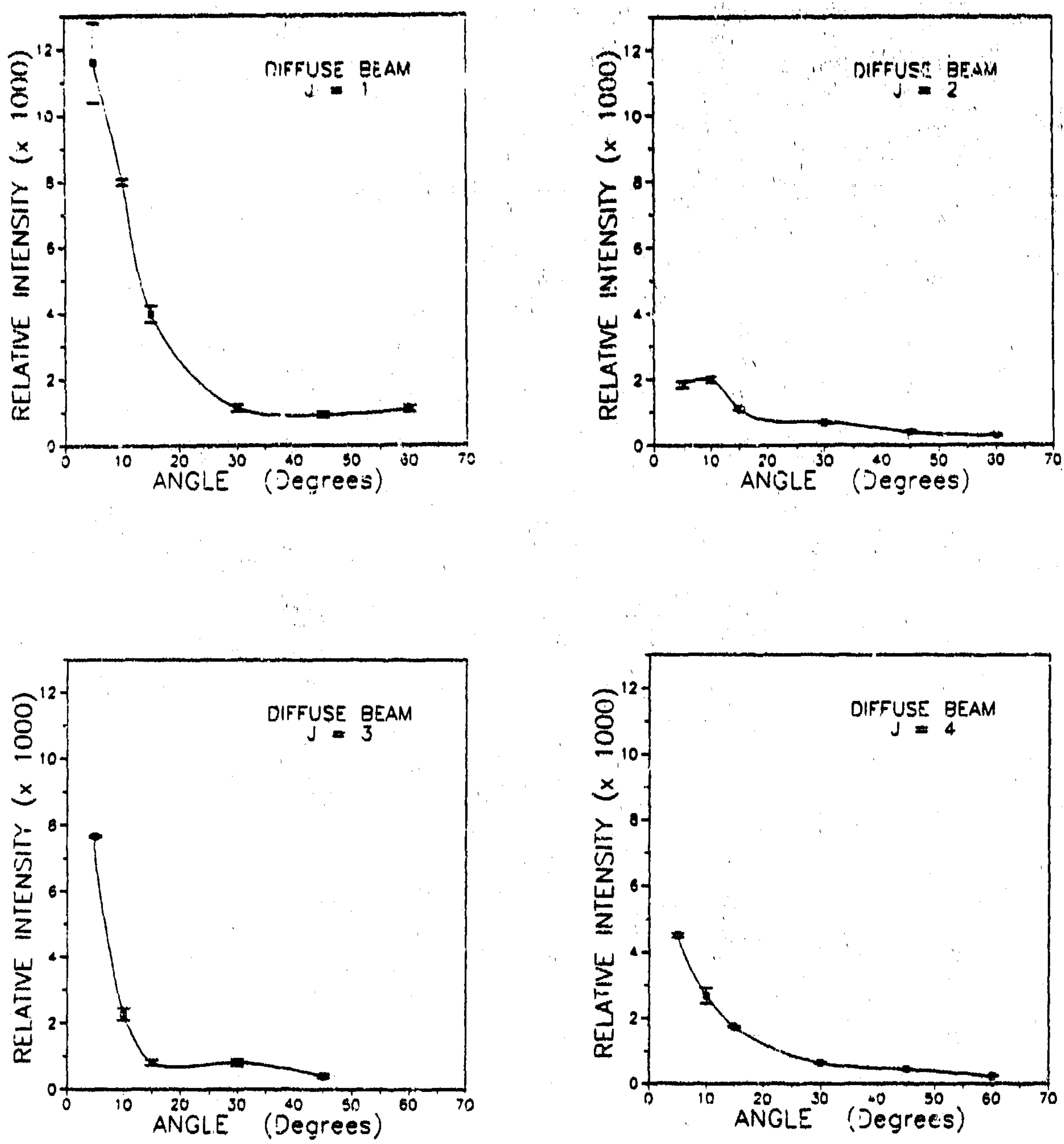

Figure 39. **First Four Harmonics of Diffuse Beam Spectrum (Full Current, Full Energy)**

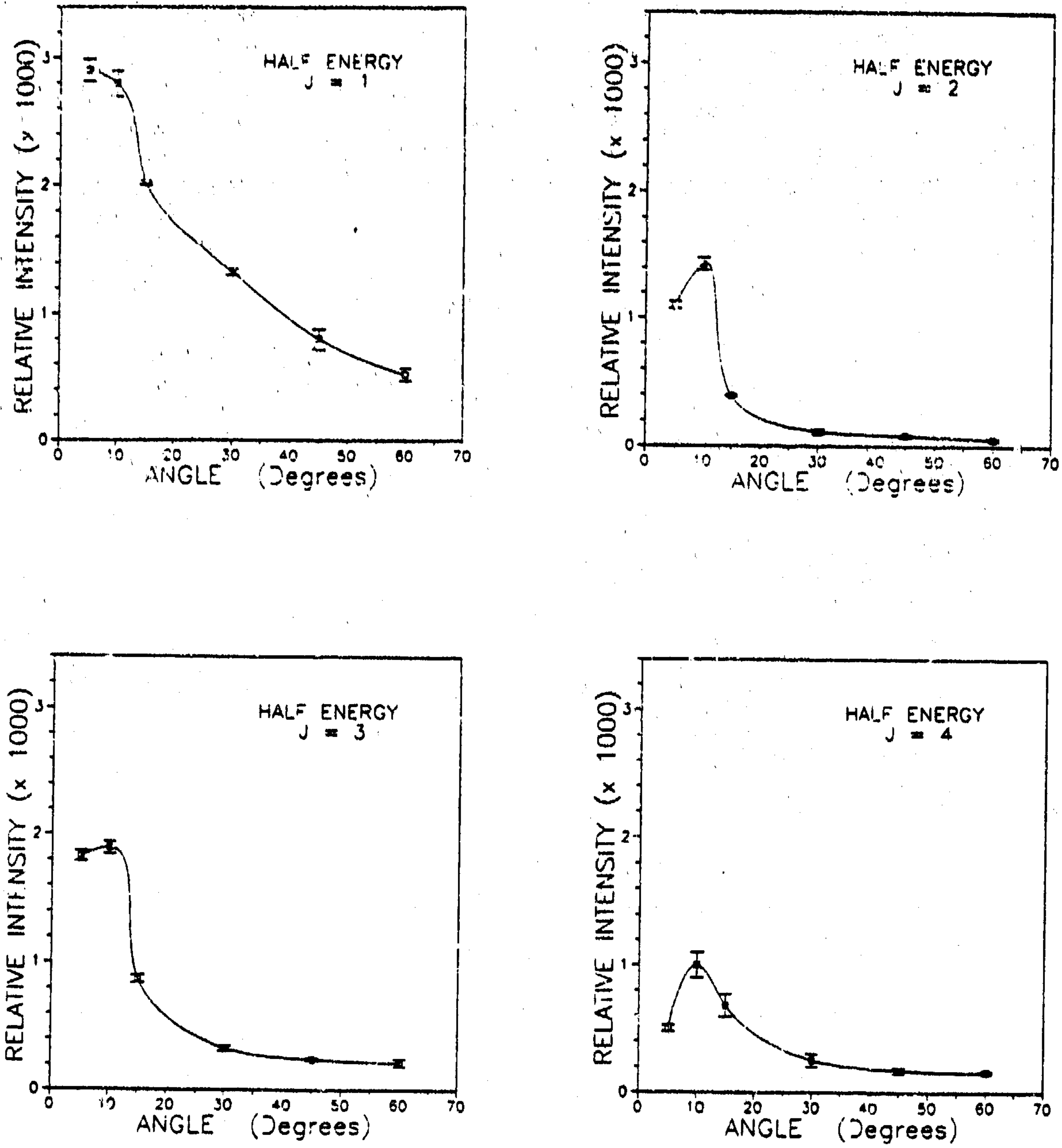

Figure 40. **First Four Harmonics of Half Energy Spectrum (Half Current)**

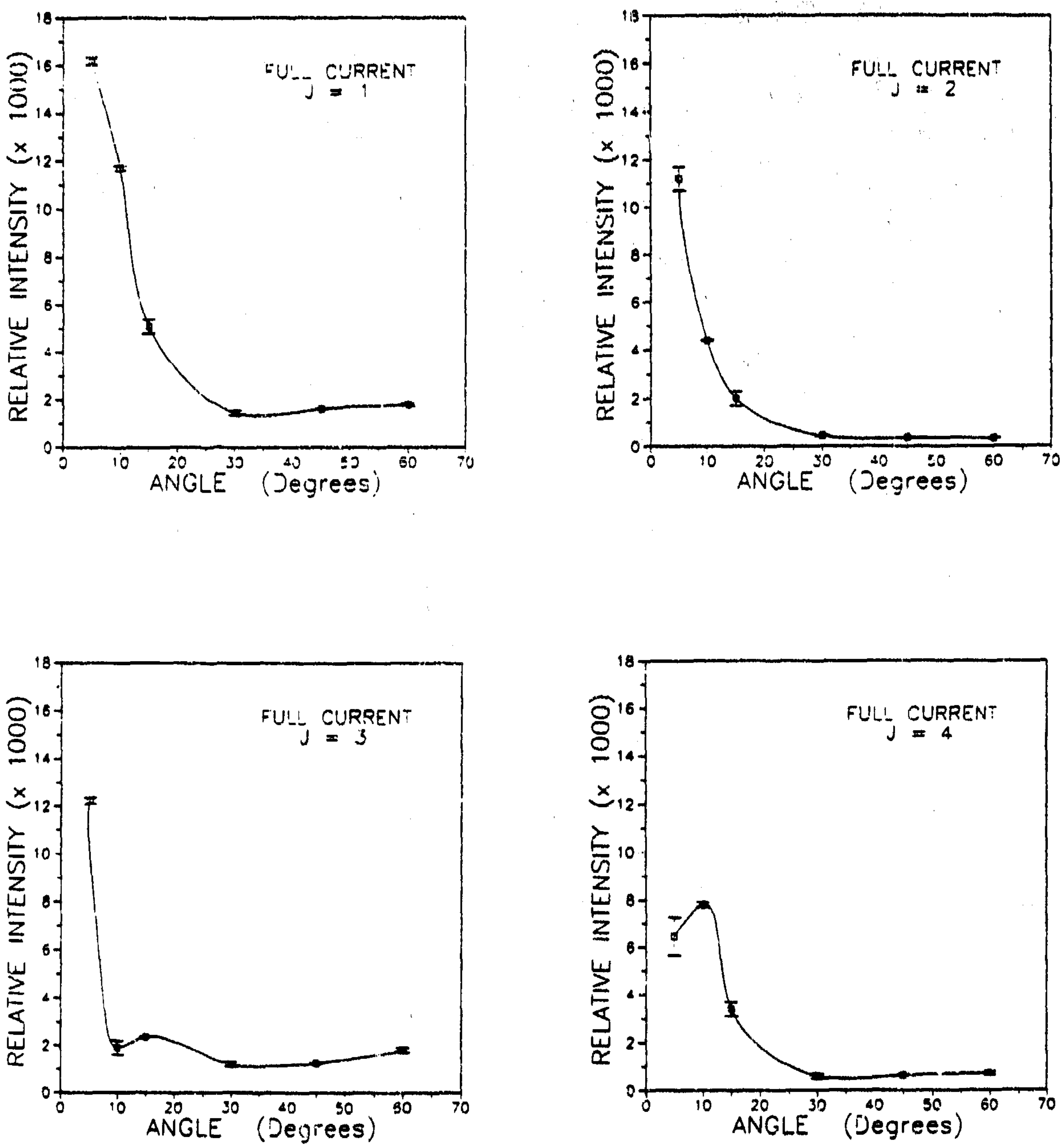

Figure 41. **First Four Harmonics of Full Current Spectrum (Full Energy)**

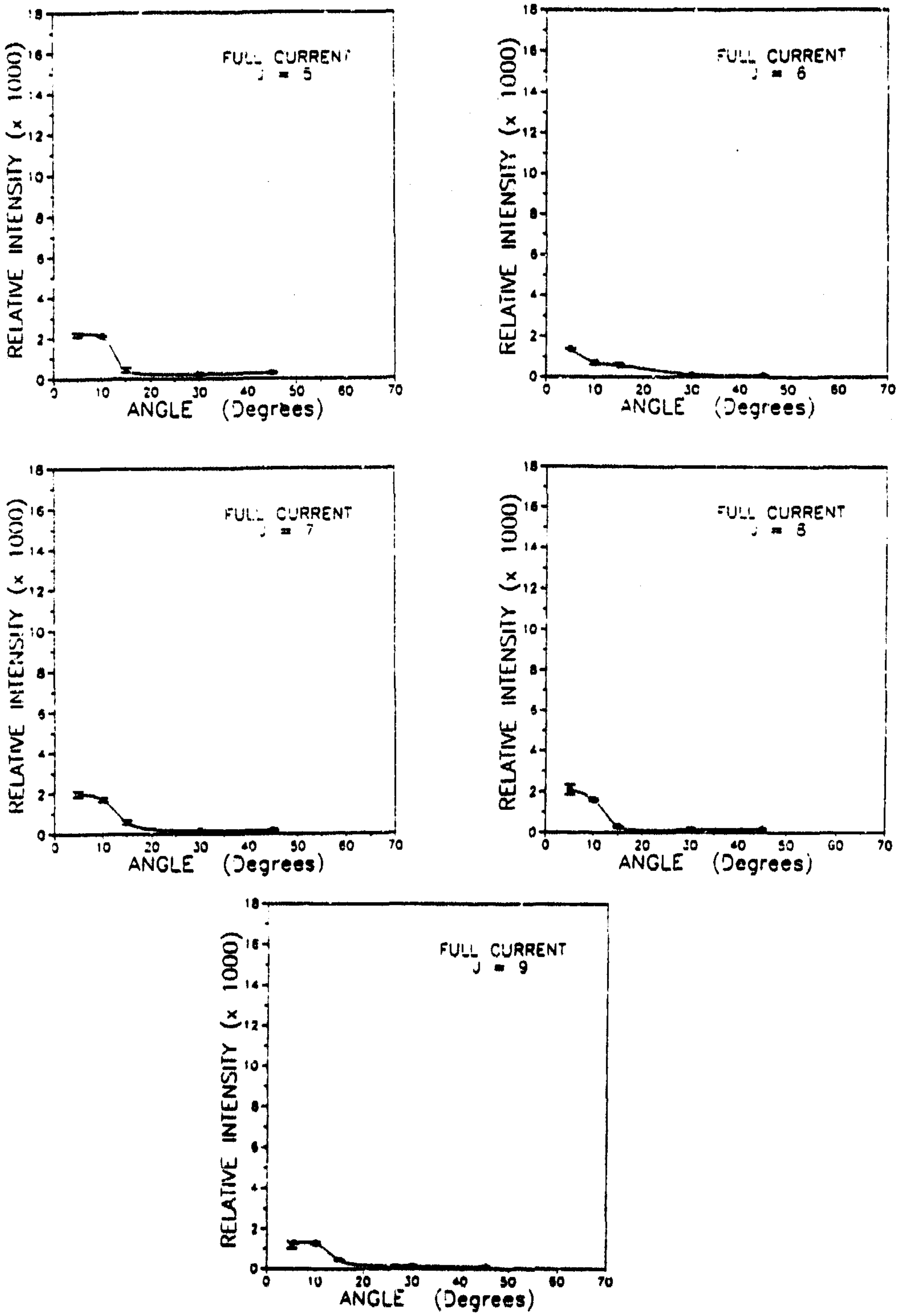

Figure 42. 5-9 Harmonics of Full Current Spectrum (Full Energy)

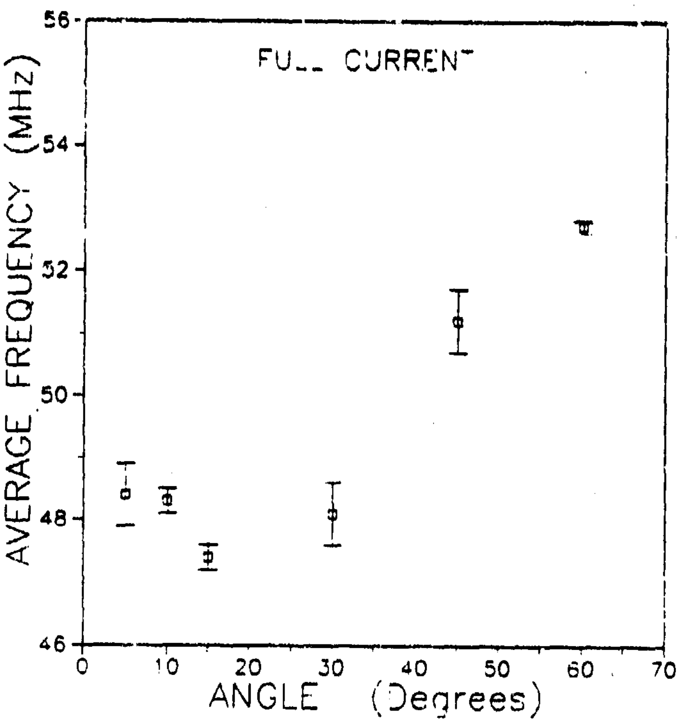

Figure 43. **Average Frequency of Spectrum for Full Current**

Figure 44) current. The same calculations were performed on the B dot spectrum, and the respective plots are in Figure 45 and 46. To determine whether shifting of the harmonic frequency had occurred, the B dot full current average frequency (Figure 45) was subtracted from the full current average frequency (see Figure 47). Similarly, the difference was evaluated and plotted for the half current values (Figure 48).

5. Modulation of Spectrum

The FFT results of the B dot are similar to the results of the pattern seen from a diffraction grating in optics. From optics [Ref. 21], the

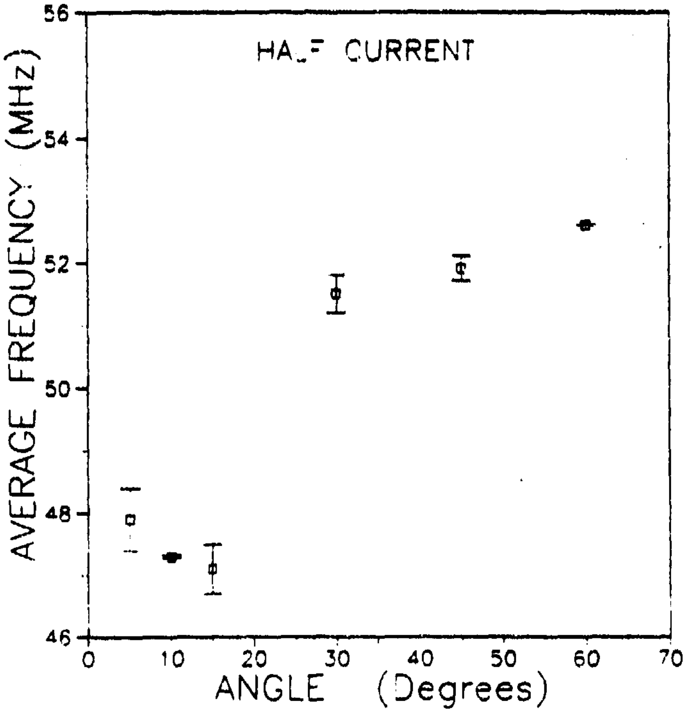

Figure 44. **Average Frequency of Spectrum for Half Current**

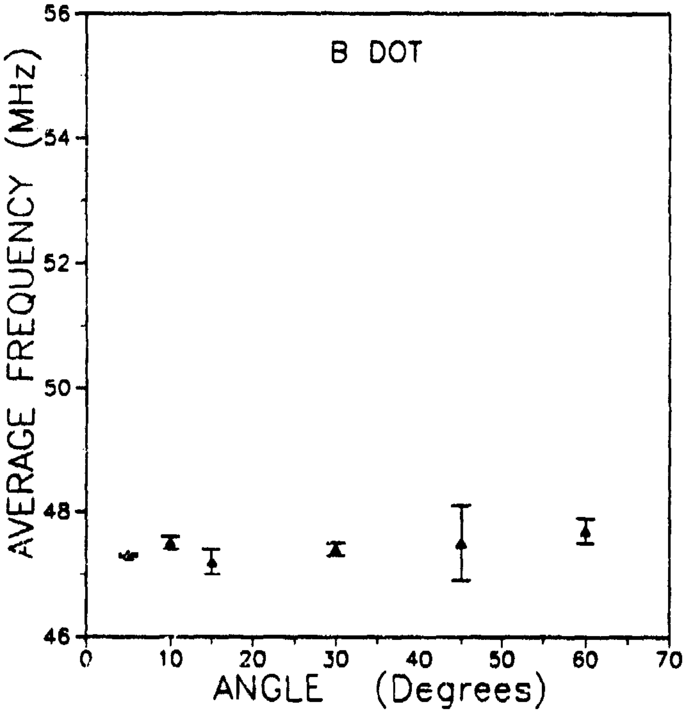

Figure 45. **Average Frequency of Spectrum for Full Current B Dot**

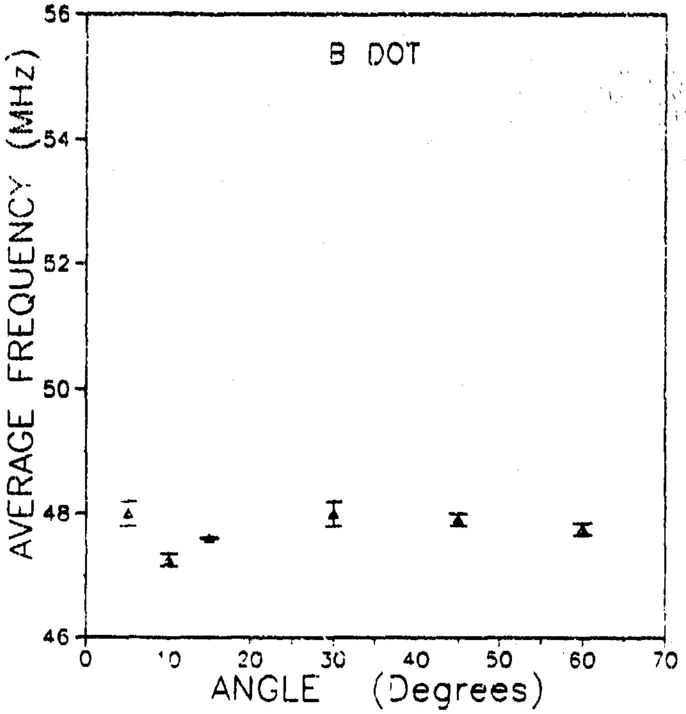

Figure 46. **Average Frequency of Spectrum for Half Current B Dot**

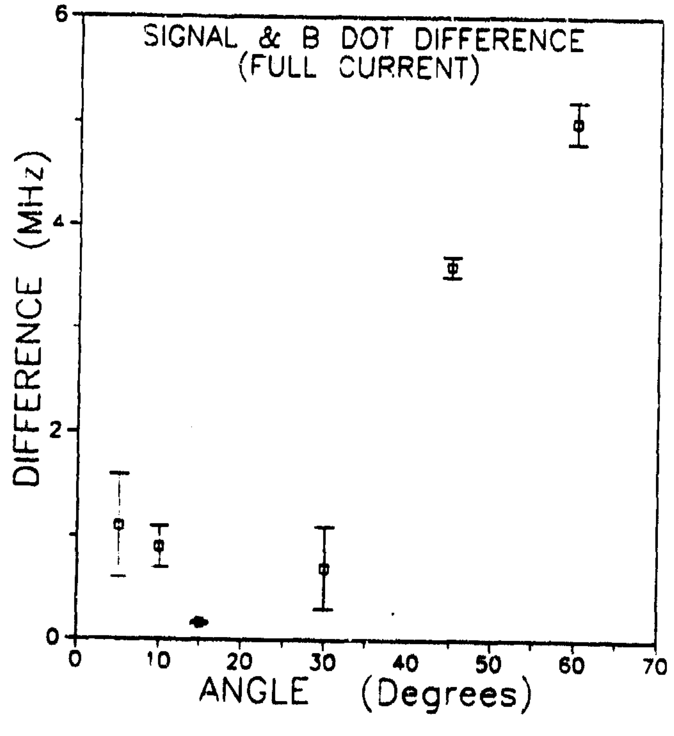

Figure 47. **Signal and B Dot Difference for Full Current**

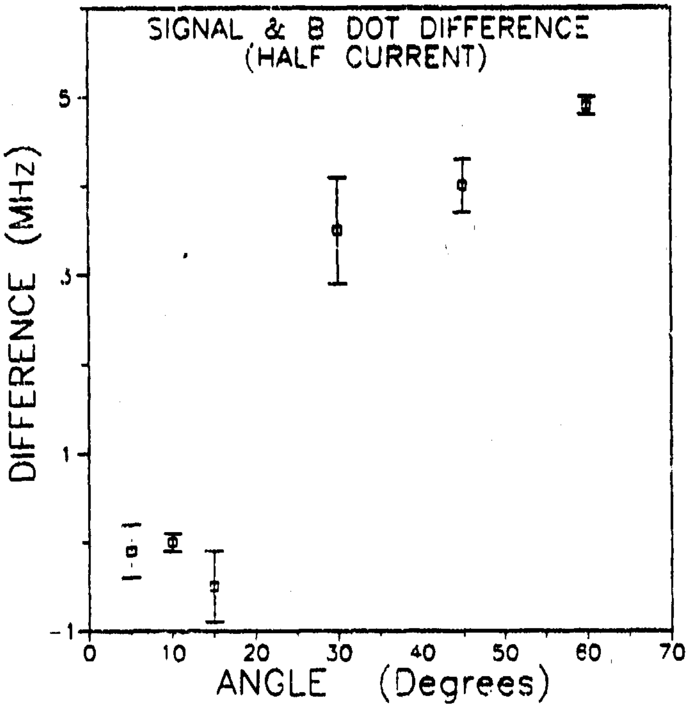

Figure 48. **Signal and B Dot Difference for Half Current**

slit width is related to the modulated minimum; the modulated minima will increase as the slit width decreases. For a single slit experiment, the modulation minima appears at the frequency ν given by

$$\nu = \frac{c}{d} \tag{10}$$

where c is the speed of light and d is the slit width or pulse width. A clear example of modulation is observed in Figure 49. Here, a simulated B dot pulse is formed by seven equal-volt 2.6 ns pulses separated by 20 ns. In this case, the pulse width (2.6 ns) acts as the slit width and is related to the modulation minima. The corresponding minimum is therefore the reciprocal of 2.6 ns, which is 385 MHz. The 20 ns pulse separation forms the 50 MHz peaks and higher harmonics.

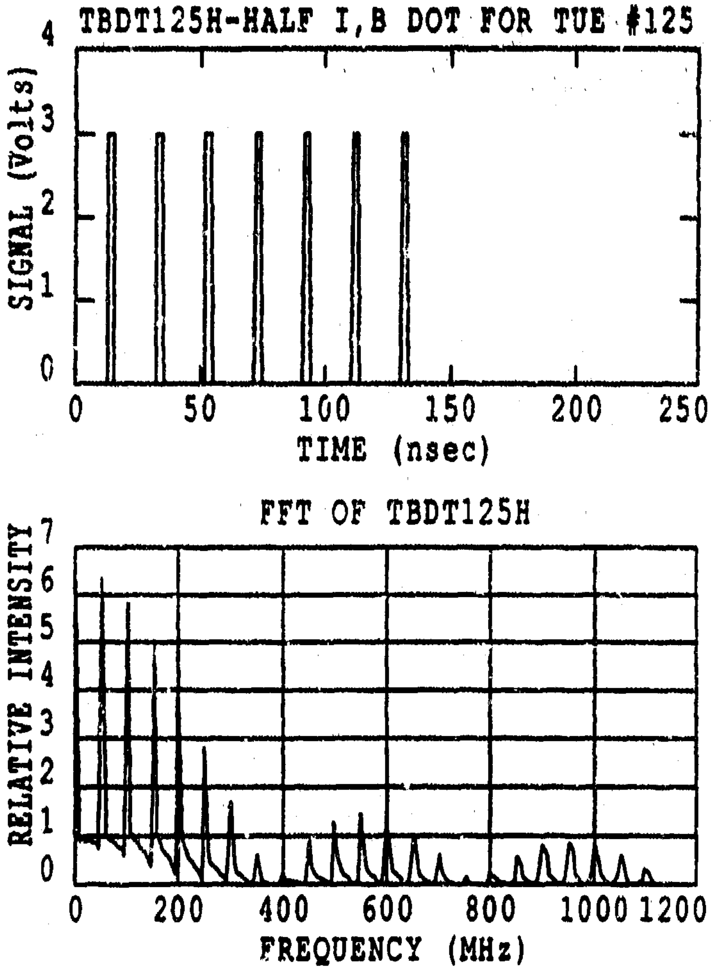

Figure 49. **Modulation Example from a Perfectly Pulsing Accelerator**

Modulation minima were also observed in the actual spectrum of the signal and B dot. An actual B dot and its spectrum are seen in the top right section of Figure 24. Although the beam is not perfect, it exhibits similar modulation minima at a slightly lower frequency (360 MHz). Table 5 lists first, second, and third modulation minima for various angles and beam parameters. These values have up to a five percent margin of error. In addition, only those signals listed in Table 5 had clear enough modulation minima to discern a value.

TABLE 5

MODULATION MINIMA

Beam Parameter	Source/ Angle	1st Minimum	2nd Minimum	3rd Minimum
Full Current	B Dot	275	525	750
	5°	270	450	610
	B Dot	275	580	905
	10°	280	–	–
	B Dot	285	595	890
	60°	290	600	895
Half Current	B Dot	360	705	895
	15°	320	675	–
	B Dot	275	500	720
	60°	295	600	895
Half Energy	B Dot	220	470	740
	5°	220	475	720
	B Dot	220	470	740
	10°	240	450	650
	B Dot	230	505	795
	15°	235	495	755
	B Dot	–	445	860
	30°	–	440	815
	B Dot	–	445	795
	60°	–	450	740

B. DISCUSSION

The five areas outlined in the results section will now be discussed. Some areas overlap and are inserted wherever clarification is necessary.

1. Signals and Related Spectrum

There are a number of general observations which hold for all signals independent of antenna angle or beam parameter. First, the overall pulse train length of the radiation signal and the B dot signal are essentially equal. Second, since the radiation depends on the rate of change of the current, there is a one-to-one correspondence of B dot peaks to major radiation signal oscillations. One can also observe the successive differences in B dot pulse peaks as a similar difference in the successive peak oscillations. Last, the 50 MHz frequency and higher harmonics are clearly evident in all radiation spectra. However, the diffuse beam radiation spectrum harmonics were less consistent and distinguishable. Also, the modulation minima of the diffuse beam were not clearly evident from the spectrum.

2. Signal Strength as a Function of Angle

By viewing Figures 32, 33, and 34, one discovers a general decrease in signal strength with increase in angle. This effect is mainly attributed to transition radiation. A comparison of the general transition radiation pattern (Figure 3) and the radiation (Figures 32–34) observed from this experiment shows significant similarities. Actual electric field strength from Table 4 is comparable to the expected strength at angles of 15 degrees or greater. However, at smaller angles, the actual electric field is considerably larger. This increase in field strength may be attributed to diffracted Cherenkov radiation and diffracted transition radiation. A closer look at the 5- and 10-degree values of both curves on Figure 34 shows a large difference at these angles. The full energy (29.5 MeV) is above the energy to cause Cherenkov radiation, and the half energy (15 MeV) is below the required energy. The ratio from Figure 37 at small angles also suggests diffracted Cherenkov radiation may be present.

The ratio of the full current peak-to-peak signal versus the half current peak-to-peak signal (Figure 35) exhibits (with the exception of the 10-degree data point) a fairly constant ratio of approximately 1.4. On re-examining equation 6, one finds that the ratio of full versus half current signals at the same angle is merely the ratio of the currents. All other values in equation 6 remain constant and, therefore, from Table 5 the average ratio of full to half currents is approximately 1.6.

In Figure 33, a propagating (tight) beam and a non-propagating (diffuse) beam are compared. Again, one observes a similar transition radiation pattern. Looking again at Figure 36, one notices a small ratio (of approximately 2) for the smaller angles and a larger ratio (of approximately 8) for the larger angles. It appears that a non-propagating beam still has significant radiation in the forward direction but radiates significantly less than a propagating beam in the other directions.

3. Relative Intensity of Spectrum Harmonics

As previously mentioned, the 50 MHz harmonics are readily observable in the radiation spectrum. Figure 38-41 indicate the relative intensity of 50 MHz (J = 1) and the next three higher harmonics. In general, the harmonic intensity follows the same pattern as the signal strength. Therefore, increases in angle cause a decrease in relative intensity. Also, each successive harmonic curve decreases in intensity. The relative intensity is still significant in higher order (sometimes up to J = 20) harmonics. This effect is seen in each signal FFT and is graphically depicted in Figure 42 with J = 5 through 9.

4. Harmonic Frequency Shift

Figures 45 and 46 indicate that a relatively constant 50 MHz beam was being produced. Viewing Figures 43 and 44, a frequency shift with increasing angle is indicated. To negate any effect changes in the beam source had on this shifting, the average B dot frequency was subtracted from the average signal spectrum frequency (Figures 46 and 47). Again, a slight shift to higher frequency with increasing angle is evident. This predicted pattern was seen earlier in Figure 2. These experimental findings seem to support the theory behind Figure 2. However, measurements in both Figures 43 and 44 involve two different collection systems. One collection system captured the signals at 5, 10, and 15 degrees, whereas the other system collected the signals at the remaining angles.

5. Modulation of Spectrum

The summary of modulated minima (Table 5) excludes minima from the diffuse beam. As mentioned previously, modulation minima were difficult to locate for diffuse beams and were consequently omitted. At larger angles, the modulation minima were easier to discern. This fact is in agreement with the Buskirk, Neighbours, and Maruyama model [Ref. 9]. From the remaining beam parameters, there is significant agreement between the B dot and signal spectrum minima. In general, the first and sometimes the second minima are consistent. The first minima appears on the average at 235 MHz for a five-pulse beam, 280 MHz for a six-pulse beam, and 340 MHz for a seven-pulse beam. Using equation 10 and multiplying by the respective number of beam pulses consistently gives values between 3.4 and 3.6 ns. These values are very close to the actual value of the beam pulse width (3.5 ns).

V. CONCLUSIONS

Radio frequency radiation, produced by the electron beam of the PHERMEX accelerator, consisted mainly of transition radiation (EMP) and minor contributions from diffracted Cherenkov radiation (when at full energy). Regardless of the beam energy, current, or frequency, the following general observations can be made concerning the analyzed radiation and its associated spectrum:

1. There is a one-to-one relation between the radiation oscillating peaks and the electron beam pulses.
2. The length of the radiation pulse train remained constant and consistent with the beam pulse train.
3. PHERMEX operating frequency of 50 MHz was consistently observed with up to the 20th harmonic in the signal spectrum.
4. In addition, there is some evidence that shifting may occur to the fundamental frequency and its harmonics in the signal spectrum. Increasing angle seems to cause an increase in the average harmonic.
5. Electric field strength of the radiation is proportional to the beam current.
6. Modulation minima of radiation signal spectrum were similar to B dot spectrum. The first modulation minima is directly related to the beam pulse width.

In addition, differences between propagating and non-propagating beams were noted as follows:

1. Propagating beams retain significant beam characteristics through their spectrum, whereas non-propagating beams do not.
2. Non-propagating beams produce less radiation in the forward direction than a propagating beam.

3. A significant decrease in radiation exists between propagating and non-propagating beams in other than the far forward direction.

There has been a major improvement in the collection system. Signals can now be quickly digitized and stored in a computer for later analysis. Previous experiments resulted in only analog measurements.

Further work, both theoretical and experimental, is already planned to continue investigating this and additional data collected during the PHERMEX experiment.

APPENDIX A

EQUIPMENT LIST

1. Tektronix 7103 Oscilloscope (3 each)
2. Transverse Electromagnetic Horn Antenna (3 each)
3. Tektronix Digitizing Camera System (DCS) (3 each)
4. Personal Computers
    - Compaq Portable II Model 4 (2 each)
    - IBM XT (1 each)
5. Video Monitors (3 each)
6. Double-Shielded Cables (3 each)
7. Tektronix Video Processor HCOZ
8. IBM Graphics Printer

APPENDIX B

IDL ANALYSIS PROGRAM

```
;This is an updated version of rf_expt by Rich Lally on 8 APR 90.

;PROGRAM TO ANALYZE RF DATA TAKEN WITH DCS
        FOR I=1,5 DO BEGIN
        PRINT,' '
        ENDFOR
PRINT,"      PROGRAM PLOTTER.PRO"                ;Program Title
PRINT,"     "
PRINT,"**** Program to analyze DCS Data. ****"
        FOR I=1,5 DO BEGIN                      ;Skips 5 lines
        PRINT,' '
        ENDFOR

READ,'DO YOU WISH TO FIND MAXIMUMS ? 1 FOR YES AND 2 FOR NO',FMAX


PRINT,"File MUST NOT have an .ASC extension."
;============ INPUT OF FILENAME =======================================
       NAME=''
READ,'Enter the name of the data file',NAME     ;Resets file name to null
                                                ;Set
        FOR JJ=1,2 DO BEGIN


        NAMELEN=STRLEN(NAME)                    ;Measures length of file name


        IF JJ EQ 2 THEN STRPUT,NAME,'BDT',1     ;INPUTS CORESPONDING BDT NAME
        TITLE=STRMID(NAME,0,(NAMELEN))          ;Strips off directory & .asc

        DAYLETTER=STRMID(TITLE,0,1)
            CASE DAYLETTER OF
             'M':     DAY='MON'
             'T':     DAY='TUE'
             'W':     DAY='WED'
             'H':     DAY='THU'
             'F':     DAY='FRI'
             ELSE:    DAY='UNKNOWN'
            ENDCASE



        DEGREES=STRMID(TITLE,1,2)

        ANTENNA=STRMID(TITLE,3,1)

        SHOTNUMBER=STRMID(TITLE,4,3)

        CURRENTL=STRMID(TITLE,7,1)

            CASE CURRENTL OF
             'F':     CURRENT='FULL'
             'H':     CURRENT='HALF'
             ELSE:    CURRENT='UNKNOWN'
            ENDCASE

          IF DEGREES EQ 'BD' THEN TOPLINE=TITLE + '-' + CURRENT + ' I,' $
          + 'B DOT FOR '+DAY + ' #' + SHOTNUMBER ELSE $
          TOPLINE=TITLE + '-' + CURRENT + ' I,' + DEGREES + ' DEG,ANT ' $
                + ANTENNA + ',' +DAY + ' #' + SHOTNUMBER

          FILE = NAME + '.ASC'

;=========== READ DATA IN FILE =======================================
;This is an updated version of rf_expt by Rich Lally on 8 APR 90.

;PROGRAM TO ANALYZE RF DATA TAKEN WITH DCS
        FOR I=1,5 DO BEGIN
        PRINT,' '
        ENDFOR
PRINT,"      PROGRAM PLOTTER.PRO"                ;Program Title
PRINT,"   "
PRINT,"**** Program to analyze DCS Data. ****"
        FOR I=1,5 DO BEGIN                       ;Skips 5 lines
        PRINT,' '
        ENDFOR

READ,'DO YOU WISH TO FIND MAXIMUMS ? 1 FOR YES AND 2 FOR NO',FMAX


PRINT,"File MUST NOT have an .ASC extension."
;============ INPUT OF FILENAME ======================================
       NAME=''
READ,'Enter the name of the data file',NAME     ;Resets file name to null
                                                 ;Set
        FOR JJ=1,2 DO BEGIN


        NAMELEN=STRLEN(NAME)                     ;Measures length of file name


        IF JJ EQ 2 THEN STRPUT,NAME,'BDT',1      ;INPUTS CORESPONDING BDT NAME
        TITLE=STRMID(NAME,0,(NAMELEN))           ;Strips off directory & .asc

        DAYLETTER=STRMID(TITLE,0,1)
            CASE DAYLETTER OF
             'M':     DAY='MON'
             'T':     DAY='TUE'
             'W':     DAY='WED'
             'H':     DAY='THU'
             'F':     DAY='FRI'
             ELSE:    DAY='UNKNOWN'
            ENDCASE


        DEGREES=STRMID(TITLE,1,2)

        ANTENNA=STRMID(TITLE,3,1)

        SHOTNUMBER=STRMID(TITLE,4,3)

        CURRENTL=STRMID(TITLE,7,1)

            CASE CURRENTL OF
             'F':     CURRENT='FULL'
             'H':     CURRENT='HALF'
             ELSE:    CURRENT='UNKNOWN'
            ENDCASE

          IF DEGREES EQ 'BD' THEN TOPLINE=TITLE + '-' + CURRENT + ' I,' $
          + 'B DOT FOR '+DAY + ' #' + SHOTNUMBER ELSE $
          TOPLINE=TITLE + '-' + CURRENT + ' I,' + DEGREES + ' DEG,ANT ' $
                + ANTENNA + ',' +DAY + ' #' + SHOTNUMBER

          FILE = NAME + '.ASC'

;=========== READ DATA IN FILE ======================================
OPENR,2,FILE                                        ;Opens input file for reading

header=strarr(80,30)                                ;Dimensions string arrays
rdhdr=strarr(80,1)
DATA = FLTARR(512)
AA = ' '
                                                    ;Read in values from header


I=0
WHILE NOT EOF(2) DO BEGIN

    IF ((I GT 19) AND (I LT 532)) THEN BEGIN
       READF,2,'$(F8.6)', FF
       DATA (I-20) = FF
    ENDIF ELSE BEGIN
       READF,2, AA
       HEADER(I) = AA
    ENDELSE
       I=I + 1
ENDWHILE


POS1 = STRPOS (HEADER(6), ':') + 2
STARLBL = STRTRIM (STRMID (HEADER(6), POS1, 3), 2)
POS2 = STRPOS (HEADER(7), ':') + 2
STOPLBL = STRTRIM (STRMID (HEADER(7), POS2, 3), 2)
START = FIX(STARLBL) & STOP = FIX(STOPLBL)        ;STRING TO NUMBER CONVERSION
DELTA=STOP-START + 1
POS3 = STRPOS (HEADER(12), ':') + 2
TIMLBL = STRTRIM (STRMID(HEADER(12),POS3,20),2)
TIME = FLOAT(TIMLBL)
IF (DEGREES EQ 'BD') AND (TIME GT 5.E-9) THEN TIME = 4.34783E-10

T=indgen(delta)*time                                ;TIME DATA
;===================ATTENUATION CORRECTION===========================
DB=0
IF (DAYLETTER EQ 'M') AND (ANTENNA EQ 'A') THEN DB=100.0
IF (DAYLETTER NE 'M') AND (ANTENNA EQ 'A') THEN DB=63.1
IF (DAYLETTER EQ 'M') AND (ANTENNA EQ 'B') THEN DB=3.2
IF (DAYLETTER EQ 'T') AND (ANTENNA EQ 'B') THEN DB=10.0
IF (DAYLETTER EQ 'W') AND (ANTENNA EQ 'B') THEN DB=10.0
IF (DAYLETTER EQ 'F') AND (ANTENNA EQ 'B') THEN DB=316.2
IF (DAYLETTER EQ 'H') AND (ANTENNA EQ 'B') THEN BEGIN
       IF (SHOTNUMBER LT 019) THEN DB=10.0
       IF (SHOTNUMBER GE 019) AND (SHOTNUMBER LT 027) THEN DB=100.0
       IF (SHOTNUMBER GE 027) THEN DB=316.2
ENDIF ELSE BEGIN
       IF (DEGREES EQ 'BD') THEN DB=70.711
ENDELSE
;==================================================================

close,2

         !xtitle='TIME (nsec)'
         !ytitle='SIGNAL (Volts)'
         !type= 16
         !MTITLE=TOPLINE
X=T*1.0E9                                           ;SCALE TO NANOSECONDS
UY=DATA(START:STOP)
Y=UY * DB                                           ;ATTENUATION CORRECTION

;===========CURSOR ROUTINE TO SIZE WAVEFORM========================
SET_PLOT,1
IF JJ EQ 2 THEN GOTO,LIFE
```

```
!C=0

PLOT,X,Y

GOTO,LIFER
LIFE: LX=X   &  LY=Y
ERASE
          !xtitle='TIME (nsec)'
          !ytitle='SIGNAL (Volts)'
          !type= 16
          !MTITLE=TOPLINE
          !XMAX=MAX(X)
!C=0
!GRID=0
!XTICKS=0

PLOT,LX,LY
LIFER:EEEEEEE=0
CURSOR,S1,S2,X1,Y1
CURSOR,S3,S4,X2,Y2
CORRECT=TIME*1.0E09
X2=X2/CORRECT
X1=X1/CORRECT
IF X1 LE 0 THEN X1 = 0.0
XXX=X(X1:X2)  &  YYY=Y(X1:X2)
DCOFFSET=Y(X1)
Y=YYY-DCOFFSET
ZEROER=X(X1)
X=XXX-ZEROER
DELTA=N_ELEMENTS(X)-1

;=========== FOURIER TRANSFORM ======================================
I=INDGEN(DELTA)
NU=1/(TIME*DELTA)                                ;FUNDAMENTAL FREQUENCY
P2=DELTA/2
FREQ=FLTARR(P2)
CDB=FLTARR(P2)

          FOR J=1,P2-1 DO BEGIN
          FREQ(J)=I(J)*NU/1.0E6                  ;IN MHZ
          BAD=WHERE ( FREQ LE 600 )   ;TO CHANGE MAX FREQ CHANGE NUMBER I.E. 600
;         BAD=WHERE ( FREQ LE 1200 )  ;TO CHANGE MAX FREQ CHANGE NUMBER I.E. 600

;==================ANTENNA CORRECTION================================

          IF DEGREES EQ 'BD' THEN GOTO,DIVE
          IF ANTENNA EQ 'A'THEN BEGIN

               CASE 1 OF
(FREQ(J) GE 1) AND (FREQ(J) LT 50): CDB(J)=((FREQ(J)-1)/(50-   $
1))*(30.1-30.0)+30.0
(FREQ(J) GE 50) AND (FREQ(J) LT 100): CDB(J)=((FREQ(J)-50)/(100-   $
50))*(30.3-30.1)+30.1
(FREQ(J) GE 100) AND (FREQ(J) LT 150): CDB(J)=((FREQ(J)-100)/(150-   $
100))*(37.9-30.3)+30.3
(FREQ(J) GE 150) AND (FREQ(J) LT 200): CDB(J)=((FREQ(J)-150)/(200-   $
150))*(41.9-37.9)+37.9
(FREQ(J) GE 200) AND (FREQ(7) LT 250): CDB(J)=((FREQ(J)-200)/(250-   $
200))*(32.1-41.9)+41.9
(FREQ(J) GE 250) AND (FREQ(J) LT 300): CDB(J)=((FREQ(J)-250)/(300-   $
300))*(30.7-32.1)+32.1
(FREQ(J) GE 300) AND (FREQ(J) LT 350): CDB(J)=((FREQ(J)-300)/(350-   $
300))*(36.0-30.7)+30.7
(FREQ(J) GE 350) AND (FREQ(J) LT 400): CDB(J)=((FREQ(J)-350)/(400-   $
350))*(34.8-36.0)+36.0
(FREQ(J) GE 400) AND (FREQ(J) LT 450): CDB(J)=((FREQ(J)-400)/(450-   $
400))*(37.3-34.8)+34.8
(FREQ(J) GE 450) AND (FREQ(J) LT 500): CDB(J)=((FREQ(J)-450)/(500-  $
450))*(38.5-37.3)+37.3
(FREQ(J) GE 500) AND (FREQ(J) LT 550): CDB(J)=((FREQ(J)-500)/(550-  $
500))*(42.5-38.5)+38.5
(FREQ(J) GE 550) AND (FREQ(J) LT 600): CDB(J)=((FREQ(J)-550)/(600-  $
550))*(39.6-42.5)+42.5

          ELSE: CDB(J)=40.0
          ENDCASE

      ENDIF ELSE BEGIN
           IF (DAY EQ 'H') OR (DAY EQ 'F') THEN GOTO,DIPPER
           IF (DAY EQ 'W') AND (SHOTNUMBER GE 008) THEN GOTO,DIPPER

            CASE 1 OF
(FREQ(J) GE 1) AND (FREQ(J) LT 50): CDB(J)=((FREQ(J)-1)/(50-  $
1))*(30.7-33.3)+33.3
(FREQ(J) GE 50) AND (FREQ(J) LT 100): CDB(J)=((FREQ(J)-50)/(100-  $
50))*(33.4-30.7)+30.7
(FREQ(J) GE 100) AND (FREQ(J) LT 150): CDB(J)=((FREQ(J)-100)/(150-  $
100))*(54.0-33.4)+33.4
(FREQ(J) GE 150) AND (FREQ(J) LT 200): CDB(J)=((FREQ(J)-150)/(200-  $
150))*(34.6-54.0)+54.0
(FREQ(J) GE 200) AND (FREQ(J) LT 250): CDB(J)=((FREQ(J)-200)/(250-  $
200))*(32.8-34.6)+34.6
(FREQ(J) GE 250) AND (FREQ(J) LT 300): CDB(J)=((FREQ(J)-250)/(300-  $
300))*(35.0-32.8)+32.8
(FREQ(J) GE 300) AND (FREQ(J) LT 350): CDB(J)=((FREQ(J)-300)/(350-  $
300))*(37.5-35.0)+35.0
(FREQ(J) GE 350) AND (FREQ(J) LT 400): CDB(J)=((FREQ(J)-350)/(400-  $
350))*(35.3-37.5)+37.5
(FREQ(J) GE 400) AND (FREQ(J) LT 450): CDB(J)=((FREQ(J)-400)/(450-  $
400))*(37.4-35.3)+35.3
(FREQ(J) GE 450) AND (FREQ(J) LT 500): CDB(J)=((FREQ(J)-450)/(500-  $
450))*(38.4-37.4)+37.4
(FREQ(J) GE 500) AND (FREQ(J) LT 550): CDB(J)=((FREQ(J)-500)/(550-  $
500))*(42.3-38.4)+38.4
(FREQ(J) GE 550) AND (FREQ(J) LT 600): CDB(J)=((FREQ(J)-550)/(600-  $
550))*(41.7-42.3)+42.3

           ELSE: CDB(J)=40.0
           ENDCASE

      ENDELSE
GOTO,FLIP
DIPPER: CASE 1 OF
(FREQ(J) GE 1) AND (FREQ(J) LT 50): CDB(J)=((FREQ(J)-1)/(50-  $
1))*(51.0-31.5)+31.5
(FREQ(J) GE 50) AND (FREQ(J) LT 90): CDB(J)=((FREQ(J)-50)/(90-  $
50))*(44.5-51.0)+51.0
(FREQ(J) GE 90) AND (FREQ(J) LT 100): CDB(J)=((FREQ(J)-90)/(100-  $
90))*(48.0-44.5)+44.5
(FREQ(J) GE 100) AND (FREQ(J) LT 200): CDB(J)=((FREQ(J)-100)/(200-  $
100))*(55.5-48.0)+48.0
(FREQ(J) GE 200) AND (FREQ(J) LT 300): CDB(J)=((FREQ(J)-200)/(300-  $
200))*(55.7-55.5)+55.5
(FREQ(J) GE 300) AND (FREQ(J) LT 400): CDB(J)=((FREQ(J)-300)/(400-  $
300))*(52.0-55.7)+55.7
(FREQ(J) GE 400) AND (FREQ(J) LT 500): CDB(J)=((FREQ(J)-400)/(500-  $
400))*(47.0-52.0)+52.0
(FREQ(J) GE 500) AND (FREQ(J) LT 600): CDB(J)=((FREQ(J)-500)/(600-  $
500))*(41.5-47.0)+47.0
(FREQ(J) GE 600) AND (FREQ(J) LT 700): CDB(J)=((FREQ(J)-600)/(700-  $
600))*(48.0-41.5)+41.5
(FREQ(J) GE 700) AND (FREQ(J) LT 800): CDB(J)=((FREQ(J)-700)/(800-  $
700))*(49.0-48.0)+48.0
(FREQ(J) GE 800) AND (FREQ(J) LT 900): CDB(J)=((FREQ(J)-800)/(900-   $
800))*(43.5-49.0)+49.0
(FREQ(J) GE 900) AND (FREQ(J) LT 1000): CDB(J)=((FREQ(J)-900)/(1000-   $
900))*(43.5-43.5)+43.5

            ELSE: CDB(J)=43.5

            ENDCASE
GOTO,FLIP
DIVE: CDB(J)=0.0
FLIP: FFF=1.0
       ENDFOR



       FREQ(0)=0.0
       IF ANTENNA EQ 'A'THEN CDB(0)=30.0
       IF ANTENNA EQ 'B'THEN CDB(0)=33.3
       BADIE=MAX(BAD)

;Z=FFT(Y,1)                                  ;WITHOUT ANTENNA RESPONSE
CT=10^(CDB/20)                               ;ANTENNA RESPONSE FUNCTION


UZ=FFT(Y,1)                                  ;WITH ANTENNA RESPONSE
Z=UZ*CT                                      ;WITH ANTENNA RESPONSE

;========== MAKE REGIS PLOT OF DATA ===============================


SET_PLOT,3
IF JJ EQ 2 THEN !NOERAS=1
!PSYM=0
IF JJ EQ 1 THEN OPENW,5,TITLE +'_COMPOSITE.PLT/None'
PLOT_TO,-5
IF JJ EQ 1 THEN SET_VIEWPORT,.08,.48,.60,.95
IF JJ EQ 2 THEN SET_VIEWPORT,.58,.98,.60,.95
!GRID=0
SCALERR = MAX(X)
!XMAX = SCALERR
!C=0
PLOT,X,Y
STOP

;====== MAKE REGIS PLOT OF FOURIER TRANSFORM =======================

!NOERAS=1



IF JJ EQ 1 THEN SET_VIEWPORT,.08,.48,.10,.45
IF JJ EQ 2 THEN SET_VIEWPORT,.58,.98,.10,.45

!GRID=1

       !MTITLE='FFT OF ' + TITLE

       !XTITLE='FREQUENCY (MHz)'
       !YTITLE='RELATIVE INTENSITY'
       SCCALER = 600                        ;TO CHANGE MAX FREQ CHANGE 600 TO
                                            ; WHATEVER FREQ
;      SCCALER = 1200
       !XMAX= SCCALER

       SPOT = SCCALER/3
       VALUE=ABS(Z(0:P2-1))

!C=0
!IGNORE=1
PLOT_IO,FREQ(0:BADIE),VALUE                ;PLOTS SEMI-LOG
;PLOT,FREQ(0:BADIE),VALUE                  ;PLOTS A LINEAR PLOT
;IF JJ EQ 1 THEN STOP

IF FMAX NE 1 THEN GOTO,FLAGGER
IF JJ EQ 1 THEN BEGIN

;==================DETERMINE MAXIMUMS=============================

READ,'USE MOUSE TO FIND MAX VALUES, BUT FIRST ENTER NUMBER OF MAXIMUMS',NMAX
      OPENW,7,TITLE + '_MAXX.DAT/LIST'
      OPENW,6,TITLE + '_MAX.DAT/LIST'
           PRINTF,7,"$('DATA VALUES OF ',A8)",TITLE
           PRINTF,6,"$('DATA VALUES OF ',A8)",TITLE
           PRINTF,7,"#   INTENSITY    FREQUENCY"
           PRINTF,7,"    _________    _________"
           PRINTF,6,"$(F8.5)",NMAX
CURSOR,Z1,Z2,X1,Y1
IF X1 LE 0 THEN X1 = 0.0

       FOR IJ = 0,NMAX-1 DO BEGIN
          WAIT,0.5
          X2=X1
          CURSOR,Z1,Z2,X1,Y1
          CORRECTO=NU
          X1=X1*1.0E6/CORRECTO
          IVAL=MAX(VALUE(X2:X1))

          PRINTF,7,'$(I2,G13.5,G13.5)',IJ,IVAL,FREQ(WHERE(VALUE EQ IVAL))
          PRINTF,6,IJ
          PRINTF,6,IVAL
          PRINTF,6,FREQ(WHERE(VALUE EQ IVAL))
       ENDFOR

       CLOSE,6
       CLOSE,7
ENDIF ELSE BEGIN

;=====================PRINT MAXIMUMS TO A FILE====================

READ,'USE MOUSE TO FIND MAX VALUES, BUT FIRST ENTER NUMBER OF MAXIMUMS',NMAX
      OPENW,4,TITLE + '_MAXX.DAT/LIST'
       OPENW,3,TITLE + '_MAX.DAT/LIST'
          PRINTF,4,"$('DATA VALUES OF ',A8)",TITLE
          PRINTF,3,"$('DATA VALUES OF ',A8)",TITLE
           PRINTF,4,"#   INTENSITY    FREQUENCY"
           PRINTF,4,"    _________    _________"
           PRINTF,3,"$(F8.5)",NMAX

CURSOR,Z1,Z2,X1,Y1
IF X1 LE 0 THEN X1 = 0.0
       FOR IJ = 0,NMAX-1 DO BEGIN
          WAIT,0.5
          X2=X1
          CURSOR,Z1,Z2,X1,Y1
          CORRECTO=NU
          X1=X1*1.0E6/CORRECTO
          IVAL=MAX(VALUE(X2:X1))
          PRINTF,4,'$(I2,G13.5,G13.5)',IJ-1,IVAL,FREQ(WHERE(VALUE EQ IVAL))
          PRINTF,3,IJ
          PRINTF,3,IVAL
          PRINTF,3,FREQ(WHERE(VALUE EQ IVAL))
       ENDFOR
       CLOSE,3
       CLOSE,4
ENDELSE

FLAGGER: TRRT=0

ENDFOR
AA=.03 * MIN(VALUE)
BB=.90 * SCCALER
XYOUTS,BB,AA,STRMID(!STIME,0,11)

CLOSE,5
STOP

CLEANPLOT
ERASE

PLOT_TO,0

END
```

LIST OF REFERENCES

1. Jelley, J. V., *Cherenkov Radiation and its Applications*, pp. 1-15, Pergamon Press, Oxford, 1958.

2. O'Grady, A. J., *Cherenkov Radiation, Transition Radiation and Diffraction Transition Radiation From Periodic Bunches for a Finite Beam Path in Air*, Master's Thesis, Naval Postgraduate School, Monterey, California, 1986.

3. Ginzburg, V. L., and Tsytovich, V. N., *Several Problems of the Theory of Transition Radiation and Transition Scattering*, pp. 1-8, North Holland Publishing Company, Amsterdam, 1978.

4. Buskirk, F. R., and Neighbours, J. R., "Cherenkov Radiation and Electromagnetic Pulse Produced by Electron Beams Traversing a Finite Path in Air," *Physical Review A*, v. 3, n. 4 (October 1986).

5. Rule, D. W., and Fiorito, R. B., *The Use of Transition Radiation As a Diagnostic For Intense Beams*, Naval Surface Weapons Center Technical Report No. NSWC TR84-134, July 1984.

6. Neighbours, J. R.; Buskirk, F. R.; and Maruyama, X. K., "Cherenkov and Sub-Cherenkov Radiation from a Charged Particle Beam," *Journal of Applied Physics*, v. 61, pp. 2741-2748, November 1986.

7. Neighbours, J. R.; Buskirk, F. R.; and Saglam, A., "Cherenkov Radiation from a Finite-Length Path in a Gas," *Physical Review A*, p. 3246, August 1983.

8. Neighbours, J. R., and Buskirk, F. R., *Radiation From Intense Electron Beams Associated with the Cherenkov Mechanism*, Naval Postgraduate School Report No. NPS-61-84-010, June 1984.

9. Neighbours, J. R.; Buskirk, F. R.; and Maruyama, X. K., *Frequency Content of Coherent Cherenkov Radiation*, Naval Postgraduate School Report No. NPS-61-90-001, November 1989.

10. Frank, I., and Ginsburg, V., "Radiation of a Uniformly Moving Electron Due to its Transition from One Medium into Another," *Journal of Physics*, v. 9, p. 353, 1944.

11. Miller, L., *Transition Radiation*, Los Alamos National Laboratory, Memorandum, February 1983.

12. Buskirk, F. R.; Mack, J. M.; and Neighbours, J. R., *Radiofrequency Radiation from the PHERMEX Electron Beam-Theory*, Los Alamos Unit Report, June 1986.

13. Buskirk, F. R.; Mack, J. M.; and Pogue, E. W., *Radiofrequency Radiation from PHERMEX Beam-Distort Experiments*, Los Alamos Unit Report, July 1985.

14. Venable, D., et al., *PHERMEX: A Pulsed High-Energy Radiographic Machine Emitting X-Rays*, Los Alamos Scientific Laboratory of the University of California Report No. LA-3241, May 1967.

15. Kanda, M., "Time Domain Sensors for Radiated Impulsive Measurements," *IEEE Transactions on Antennas and Propagation*, v. AP-31, n. 3, p. 438, 1983.

16. Lawton, R. A., and Ondrejka, A. R., *Antennas and the Associated Time Domain Range for the Measurement of Impulsive Fields*, NBS Technical Note 1008, November 1978.

17. Tektronix, Inc., *DCSOI Digitizing Camera System Instruction Manual*, Beaverton, Oregon, 1986.

18. Williams, D. B., *A Technique for Digitizing Oscilloscope Voltage Versus Time Photographs for Frequency Analysis Using a Tektronix Digitizing Camera System*, Master's Thesis, Naval Postgraduate School, Monterey, California, 1986.

19. *VAX IDL User's Guide*, Research Systems, Inc., Denver, Colorado, May 1988.

20. Driver, L. D., and Kanda, M., *TEM Horn Calibration*, NBS Special Test, NBS, Boulder, Colorado, May 1986.

21. Ohanian, H. C., *Physics*, pp. 880–900, W. W. Norton, New York, 1985.

INITIAL DISTRIBUTION LIST

		No. Copies
1.	Defense Technical Information Center Cameron Station Alexandria, VA 22304-6145	2
2.	Library, Code 0142 Naval Postgraduate School Monterey, CA 93943-5002	2
3.	Physics Library, Code 61 Department of Physics Naval Postgraduate School Monterey, CA 93943-5000	2
4.	Professor J. R. Neighbours, Code 61Nb Department of Physics Naval Postgraduate School Monterey, CA 93943-5000	5
5.	Professor F. R. Buskirk, Code 61Bs Department of Physics Naval Postgraduate School Monterey, CA 93943-5000	5
6.	Professor X. K. Maruyama, Code 61Xk Department of Physics Naval Postgraduate School Monterey, CA 93943-5000	2
7.	Dr. Dave Moir M4, M.S. P-940 Los Alamos National Laboratory Los Alamos, NM 87545	2
8.	LT W. Fritchie PMW 145 SPAWAR Washington, DC 20363-5100	2

9. Naval Surface Weapons Center 1
White Oak Laboratory
Attn: Dr. Eugene E. Nolting (R401)
10901 New Hampshire Avenue
Silver Springs, MD 20903-5000

10. Dr. Harold Dogliani 1
IT-4, B-232, P. O. Box 503
Los Alamos National Laboratory
Los Alamos, NM 87545

11. Chairman, Code 61 1
Department of Physics
Naval Postgraduate School
Monterey, CA 93943-5000

12. Commander 2
United States Army Element Defense Nuclear Agency
Electromagnetic Applications Division
ATTN: CPT Richard W. Lally
Alexandria, VA 20310